SUPPLEMENTARY INFORMATION

Chiral water-soluble molecular capsules with amphiphilic interiors

Arkadiusz Sakowicz, Agnieszka Szumna*

Table of content

1. Synthesis and compounds characterization

All solvents and chemicals used were purchased from Sigma Aldrich, TCI Europe N. V., Roth, Chem Impex Inc., and Euriso-top, were of reagent grade and were used without further purification.

All reactions were carried out under the atmosphere of the air.

ECD spectra were recorded on ECD Jasco J-715 spectropolarimeter.

IR spectra were recorded on SHIMADZU IRTracer100 spectrophotometer.

High-resolution mass spectra were recorded on SYNAPT spectrometer.

Optical rotations were recorded on Jasco P-2000 polarymeter.

Synthesis of (L-GluR)$_2$

Resorcin[4]arene **R**[1] (2.16 g, 3 mmol), L-glutamic acid (2.21 g 15 mmol), and formaldehyde (40 % aqueous solution, 0.36 ml, 12 mmol) were added to the mixture of DMF and water (1:3, 80 ml). The solution was heated to 60°C and stirred at that temperature for 3 days. After cooling the reaction was evaporated and the precipitate was washed with water, acetonitrile, again with water, and dried, yield: 50%. ^{1}H NMR (600 MHz, D_2O) δ 7.03 (s, 1H); 4.36 (d, *J* = 14.7 Hz, 1H); 4.27 (t, *J* = 7.8 Hz, 1H), 4.17 (d, *J* = 14.6 Hz, 1H); 4.01 (m, 1H); 3.48 (t, *J* = 6.6 Hz, 2H); 2.36 (m, 2H); 2.19 (m, 1H); 2.16 (m, 1H); 2.01 (m, 2H); 1.80 (m, 1H); 1.36 (t, *J* = 7.5 Hz, 2H); ^{13}C NMR (150 MHz, D_2O) δ 179.5; 178.9; 150.2; 150.1; 125.4; 124.2; 112.1; 63.0; 61.6; 61.5; 36.2; 34.3; 29.9; 29.8; 29.3; 23.1. IR (KBr): ν/cm^{-1} 3315; 2942; 1874; 1730; 1644; 1230; 658. Optical rotation: $[\alpha]_D$ = 18.0 (c = 9.99 mg / ml, H_2O, pH = 4.8, 22.7 °C). HRMS (ESI-TOF): calcd m/z for $C_{64}H_{75}N_4O_{24}$ [M-H]$^-$ 1283.4771 found 1283.4757.

Synthesis of (L-ArgR)$_2$

L-Arginine monohydrochloride (0.44 g 2.01 mmol) was dissolved in water (pH 3.5, 5 ml). Further, methanol (5 ml), resorcin[4]arene **R** (0.30 g, 0.41 mmol) and formaldehyde (40 % aqueous solution, 0.12 ml, 1.64 mmol) were added. The solution was heated to 60°C and stirred at that temperature for 1 day. After cooling the reaction was evaporated to dryness and the product was purified on the Sephadex LH-20 column, yield: 47%. ^{1}H NMR (600 MHz, D_2O) δ 7.26 (s, 1H); 4.27 (t, *J* = 7.8 Hz, 1H); 4.15 (d, *J* = 13.2 Hz, 1H), 4.04 (d, *J* = 13.1 Hz, 1H); 3.48 (t, *J* = 6.3 Hz, 2H); 3.41 (t, *J* = 6.0 Hz, 1H); 2.86 (t, *J* = 7.2 Hz, 2H); 2.14 (m, 2H); 1.68 (m, 2H), 1.34 (bm, 2H), 1.30 (m, 2H); ^{13}C NMR (150 MHz, D_2O) δ 173.3; 156.6; 151.0; 151.0; 126.5; 108.3; 61.5; 60.8; 41.1; 40.3; 34.2; 29.8; 29.3; 26.6; 23.8. IR (KBr): ν/cm^{-1} 3346; 3177; 2938; 2870; 1634; 1472; 1400; 1053. Optical rotation: $[\alpha]_D$ = 11.5 (c = 10.00 mg / ml, H_2O, pH = 4.8, 22.6 °C). HRMS (ESI-TOF): calcd m/z for $C_{68}H_{105}N_{16}O_{20}$ [M-H]$^+$ 1465.7691 found 1465.7704.

Synthesis of (D-GluR+L-ArgR)

To a water solution of (D-**GluR**)$_2$ (5 mg, 2 µmol, in 2 ml of water at pH 5.0) a water solution of (L-**ArgR**)$_2$ (5 mg, 1.5 µmol, in 2 ml of water at pH 5.0) was added. The precipitate was formed, which was washed with water (2 x 5 ml) and dried. The products was obtained in 82 %. IR (KBr): ν/cm^{-1} 3377; 2940; 2870; 1643; 1464; 1408; 1057; 835. Optical rotation: $[\alpha]_D$ = 111.7 (c = 10.00 mg / ml, H_2O, pH = 9.0, 22.6 °C).

Synthesis of (L-GluR+L-ArgR)

To a water solution of (D-**GluR**)$_2$ (5 mg, 2 μmol, in 2 ml of water at pH 5.0) a water solution of (L-**ArgR**)$_2$ (5 mg, 1.5 μmol, in 2 ml of water at pH 5.0) was added. The precipitate was formed, which was washed with water (2 x 5 ml) and dried. The product was obtained in 80 %. IR (KBr): ν/cm^{-1} 3381; 2938; 2868; 1645; 1458; 1055; 835. Optical rotation: $[\alpha]_D$ = 69.0 (c = 10.08 mg / ml, H_2O, pH = 9.0, 22.7 °C).

2. NMR spectra

2.1. NMR spectra of capsules

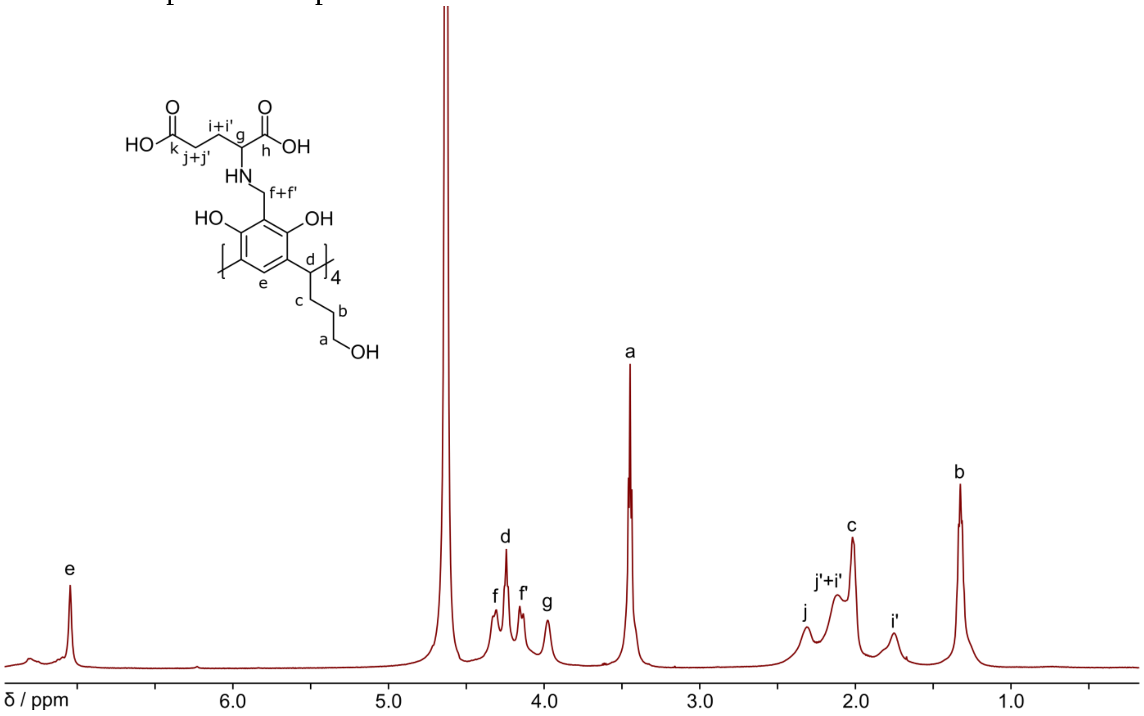

Figure S1. [1]H NMR spectrum of (L-**GluR**)$_2$ (600 MHz, 298 K, pD 4.8, D_2O, NaOD / DCl).

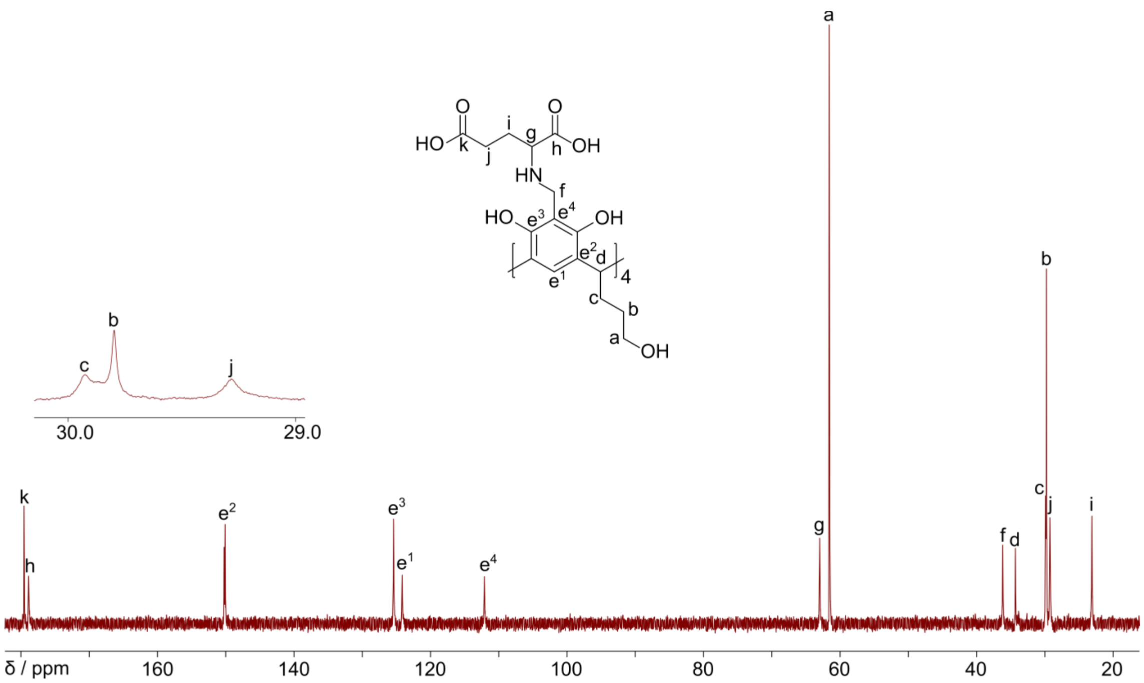

Figure S2. [13]C NMR spectrum of (L-**GluR**)$_2$ (150 MHz, 298 K, pD 4.8, D_2O, NaOD / DCl).

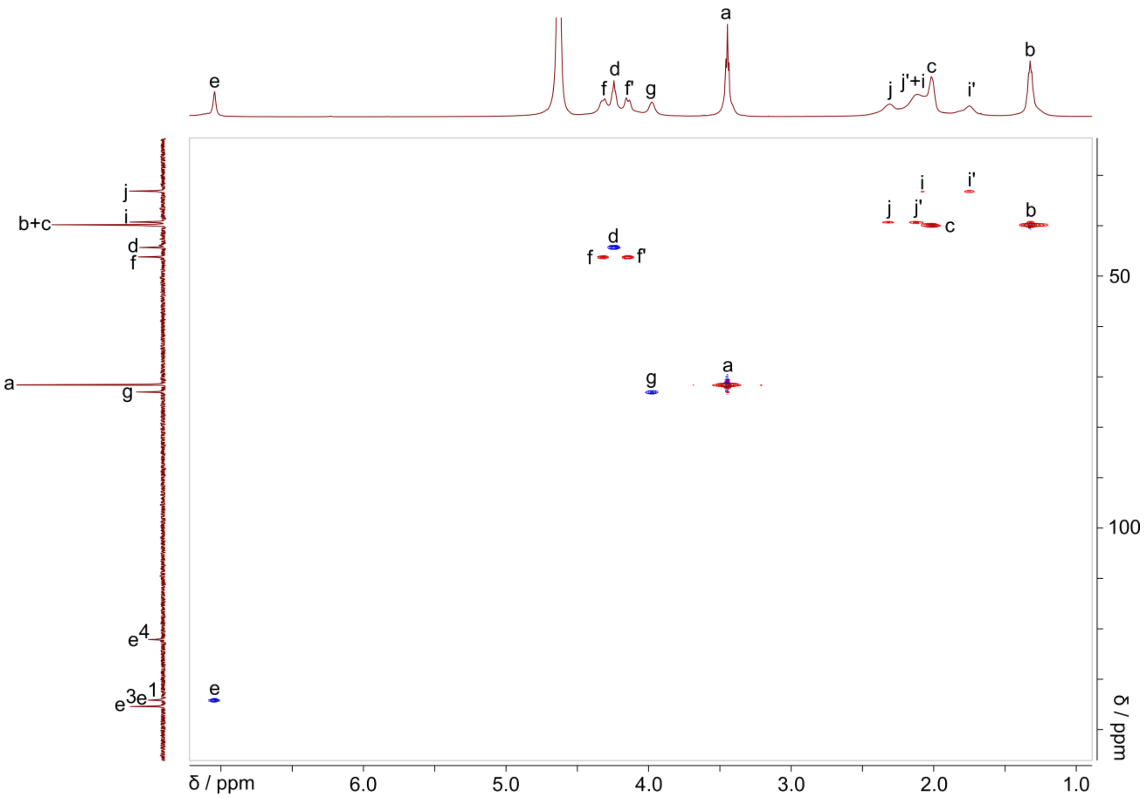

Figure S3. HSQC spectrum of (L-**GluR**)$_2$ (600 MHz, 298 K, pD 4.8, D_2O, NaOD / DCl).

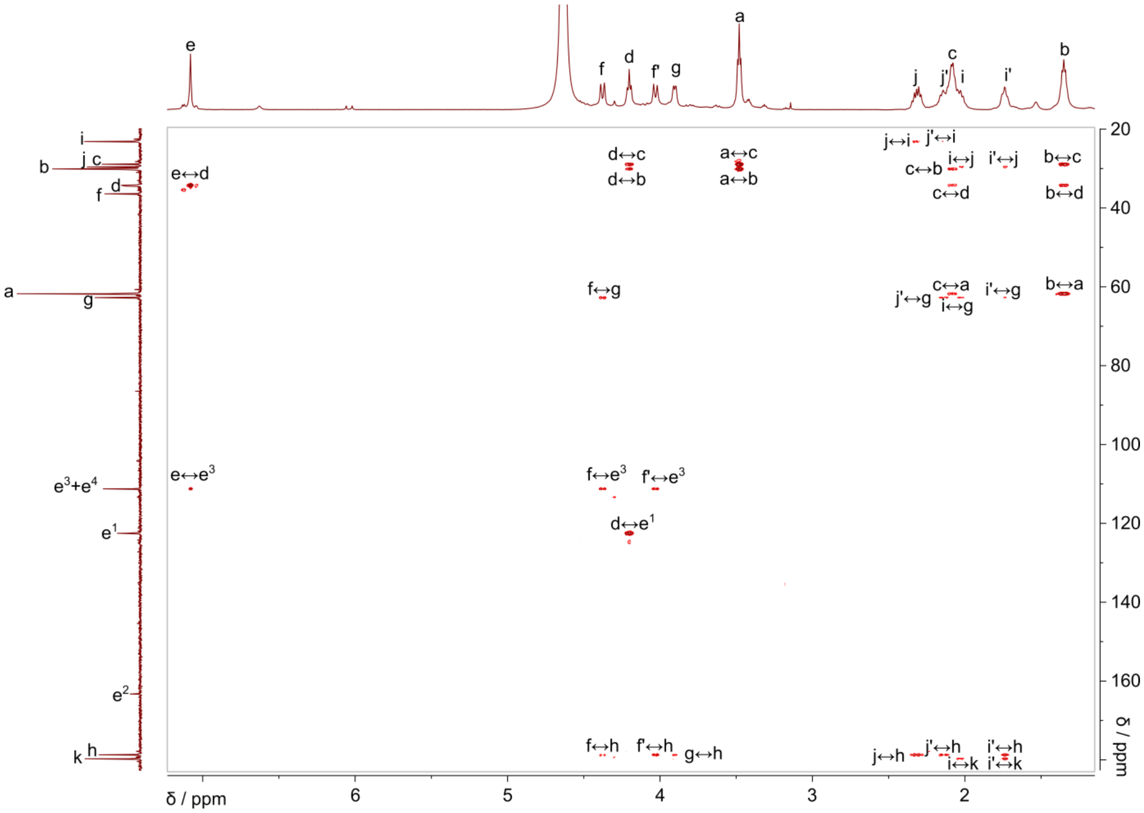

Figure S4. HMBC spectrum of (L-**GluR**)$_2$ (600 MHz, 298 K, pD 11.0, D_2O, NaOD / DCl).

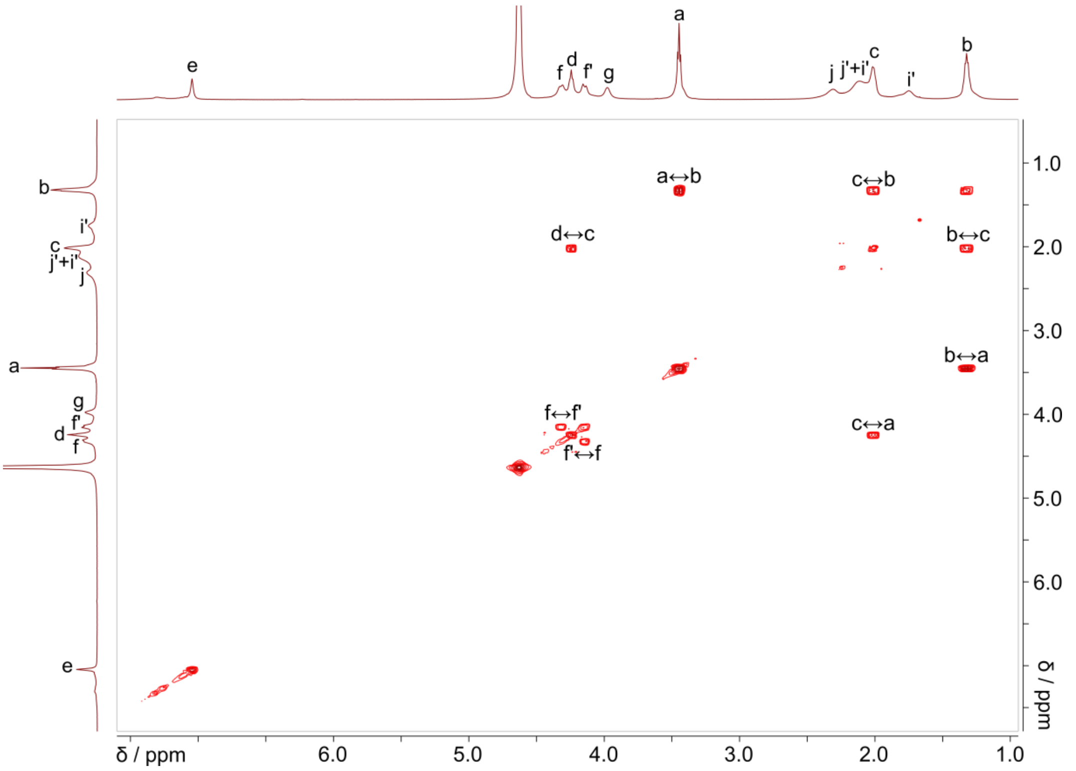

Figure S5. COSY spectrum of (L-**GluR**)$_2$ (600 MHz, 298 K, pD 4.8, D_2O, NaOD / DCl).

.

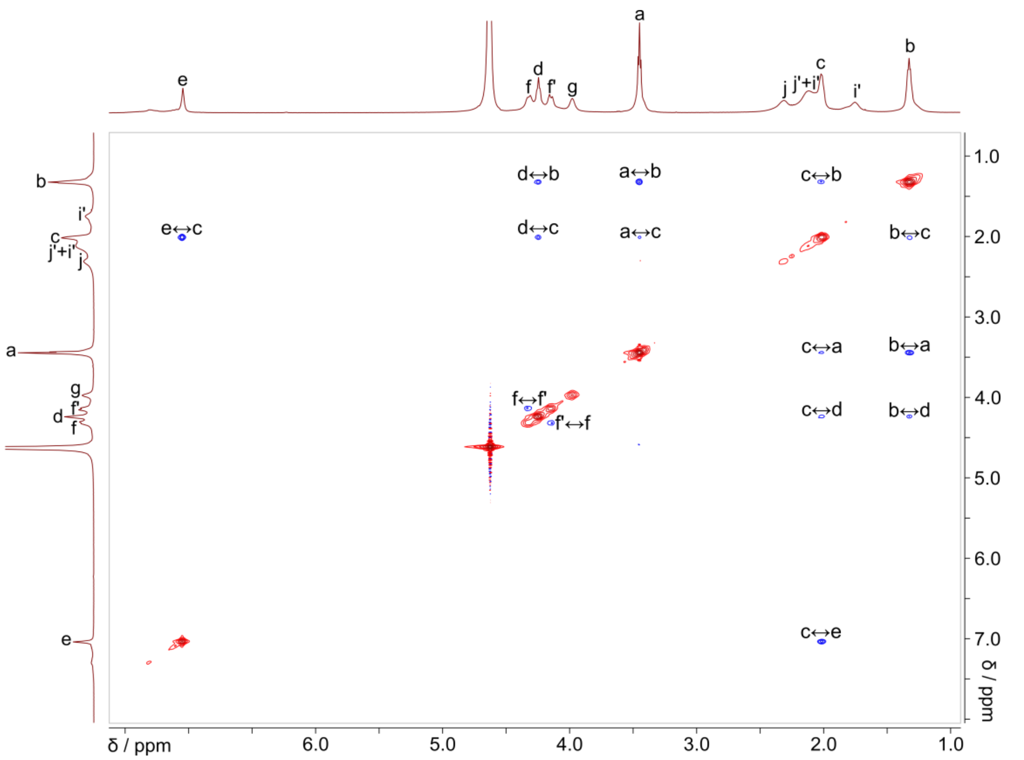

Figure S6. ROESY spectrum of (L-**GluR**)$_2$ (600 MHz, 298 K, pD 4.8, D_2O, NaOD / DCl).

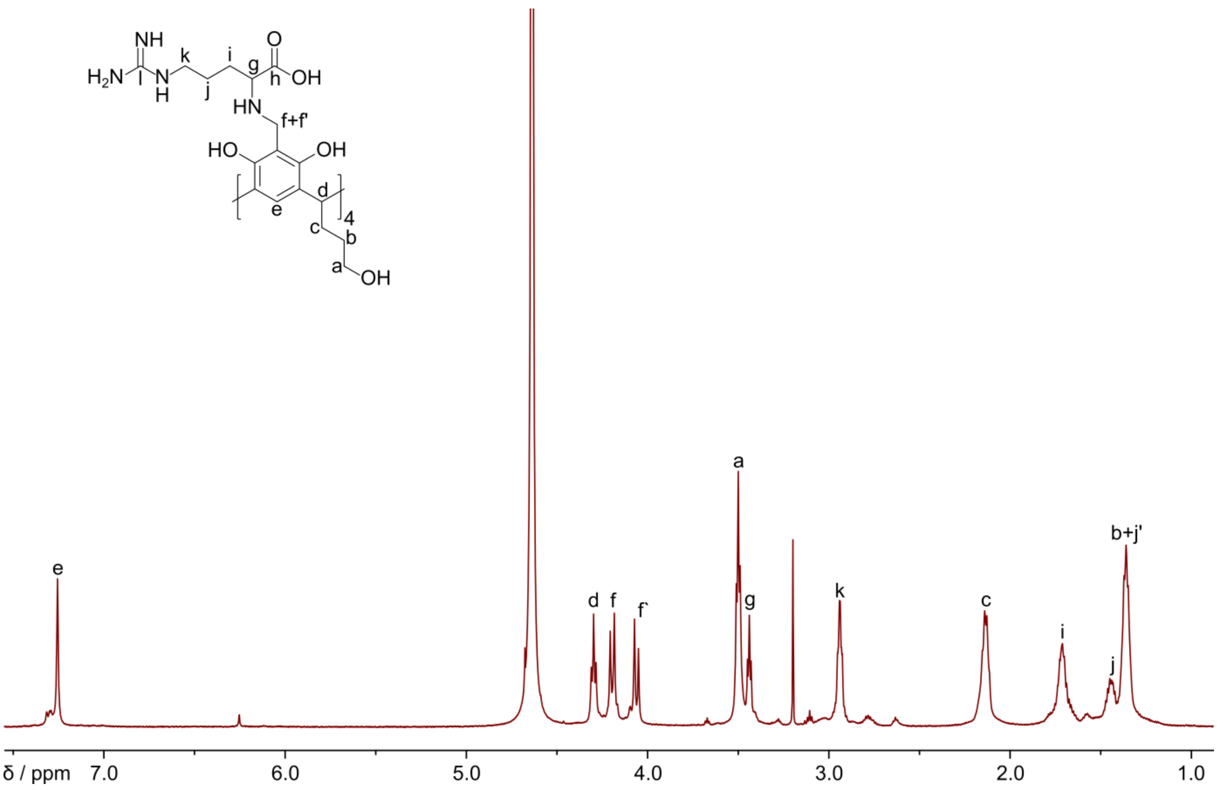

Figure S7. ^{1}H NMR spectrum of (L-**ArgR**)$_2$ (600 MHz, 298 K, pD 4.8, D_2O, NaOD / DCl).

.

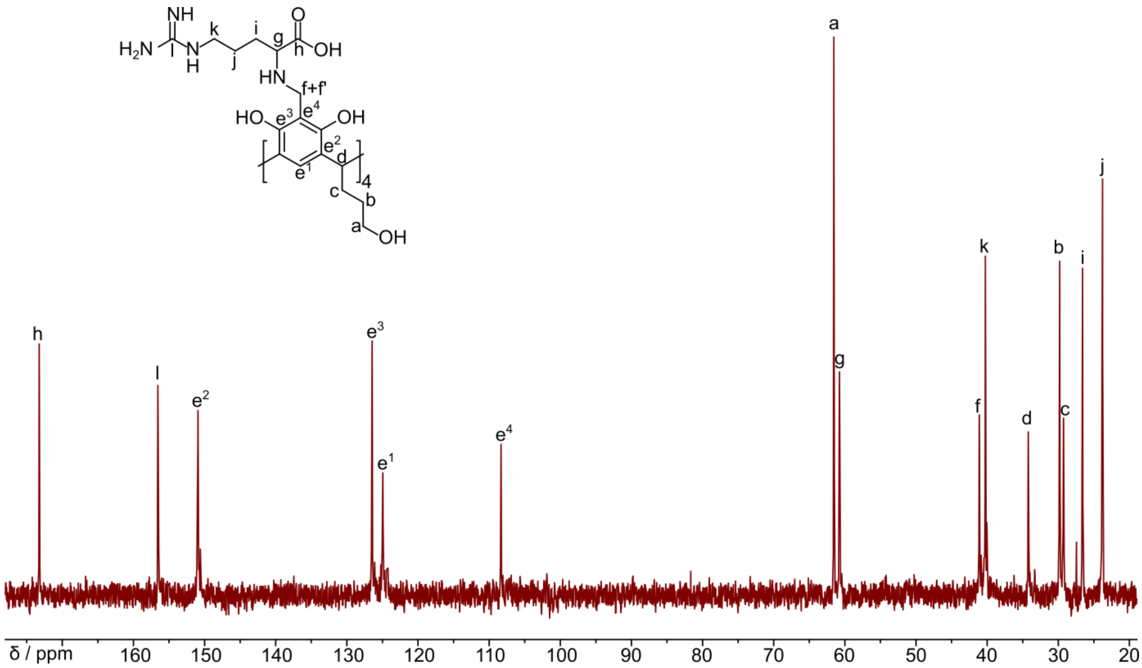

Figure S8. ^{13}C NMR spectrum of (L-**ArgR**)$_2$ (150 MHz, 298 K, pD 4.8, D_2O, NaOD / DCl).

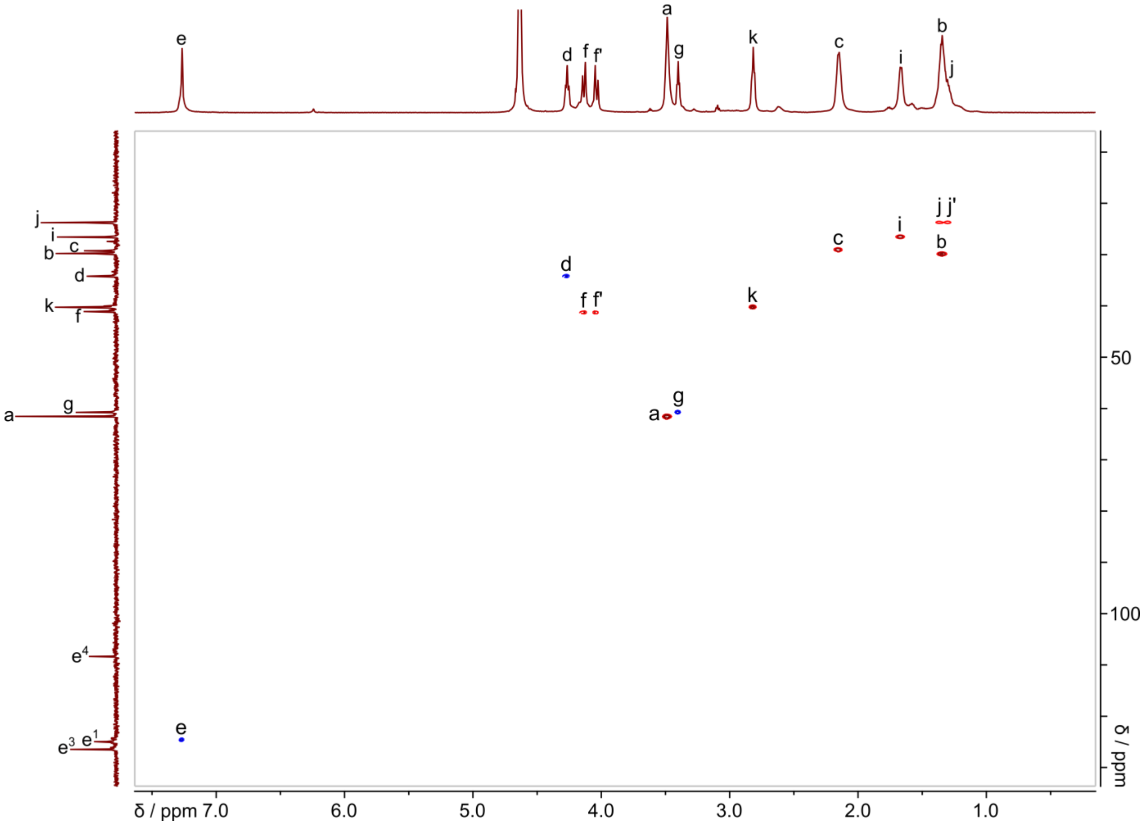

Figure S9. HSQC spectrum of (L-**ArgR**)$_2$ (600 MHz, 298 K, pD 4.8, D_2O, NaOD / DCl).

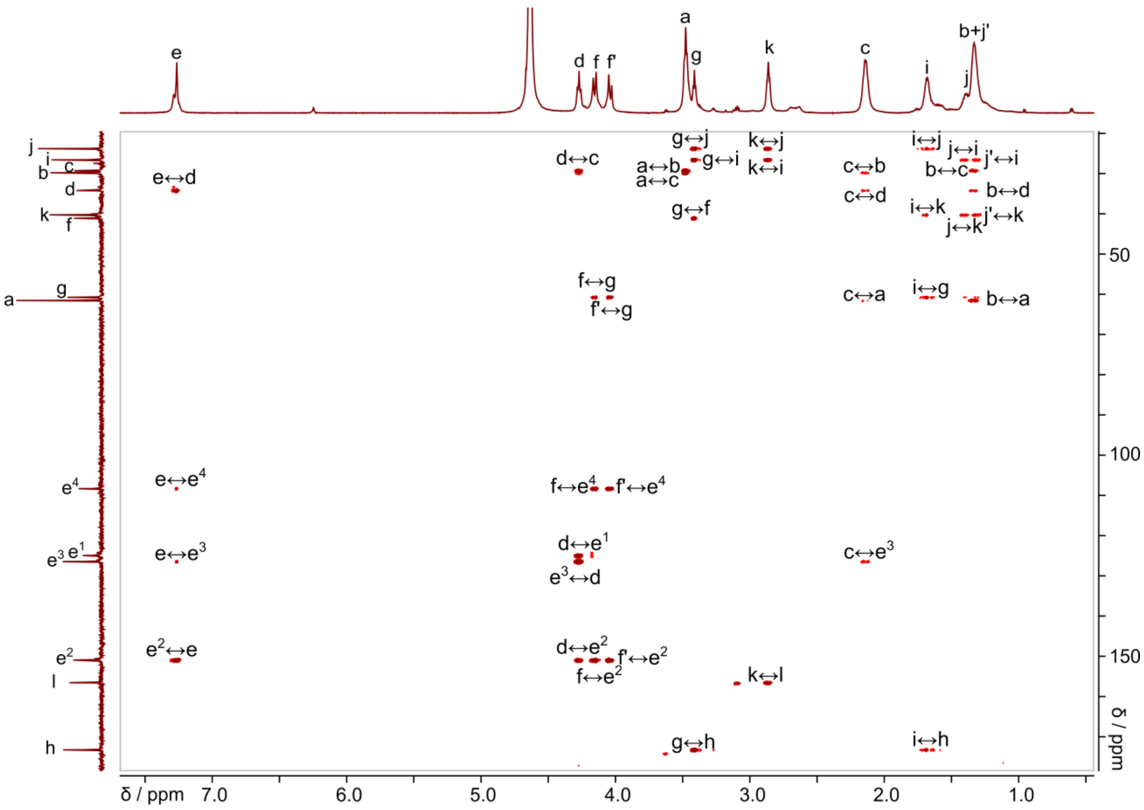

Figure S10. HMBC spectrum of (L-**ArgR**)$_2$ (600 MHz, 298 K, pD 4.8, D_2O, NaOD / DCl).

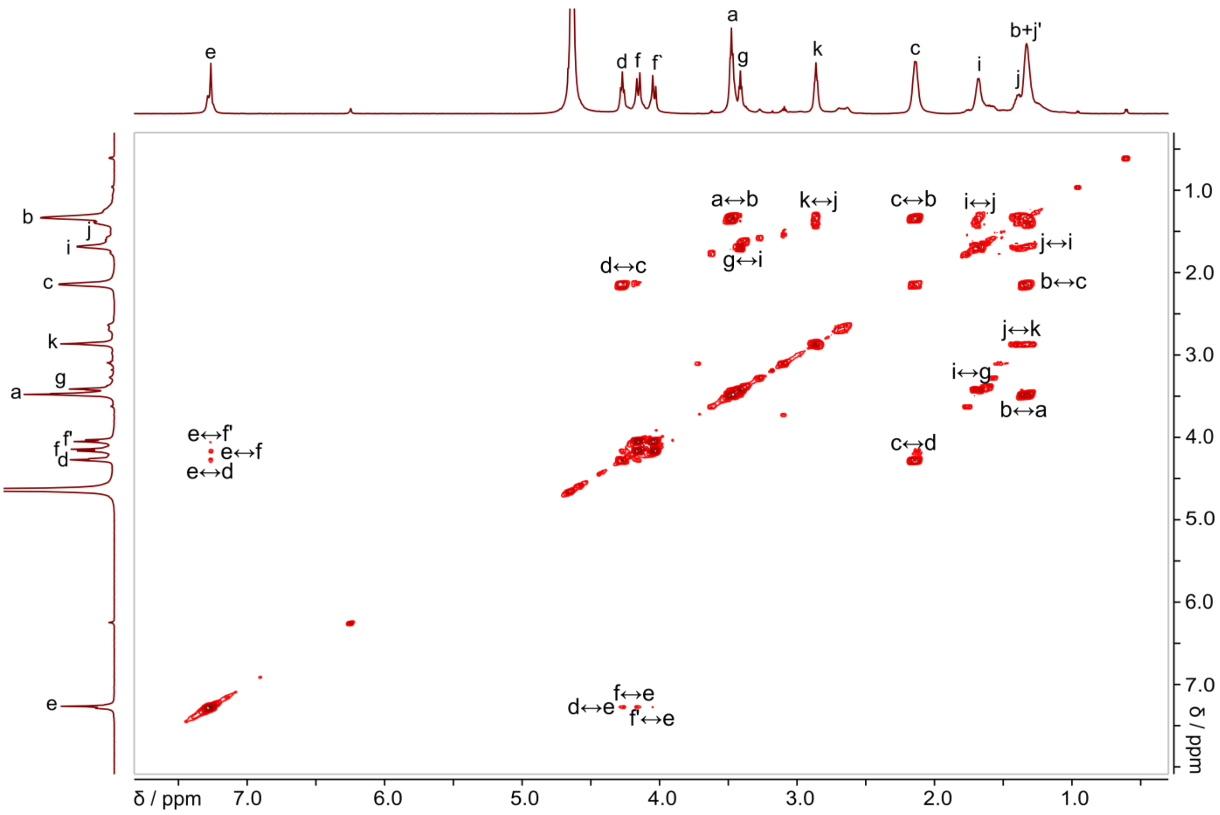

Figure S11. COSY spectrum of (L-**ArgR**)$_2$ (600 MHz, 298 K, pD 4.8, D_2O, NaOD / DCl).

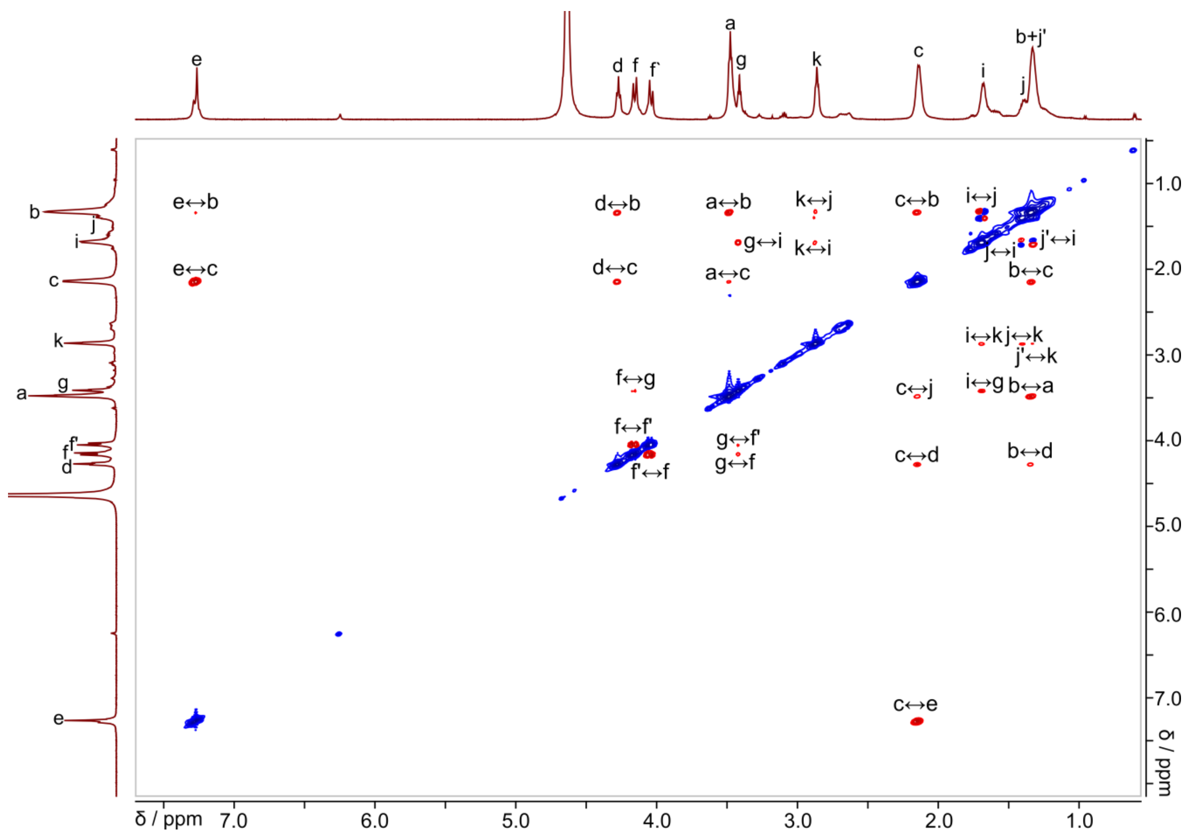

Figure S12. ROESY spectrum of (L-**ArgR**)$_2$ (600 MHz, 298 K, pD 4.8, D_2O, NaOD / DCl).

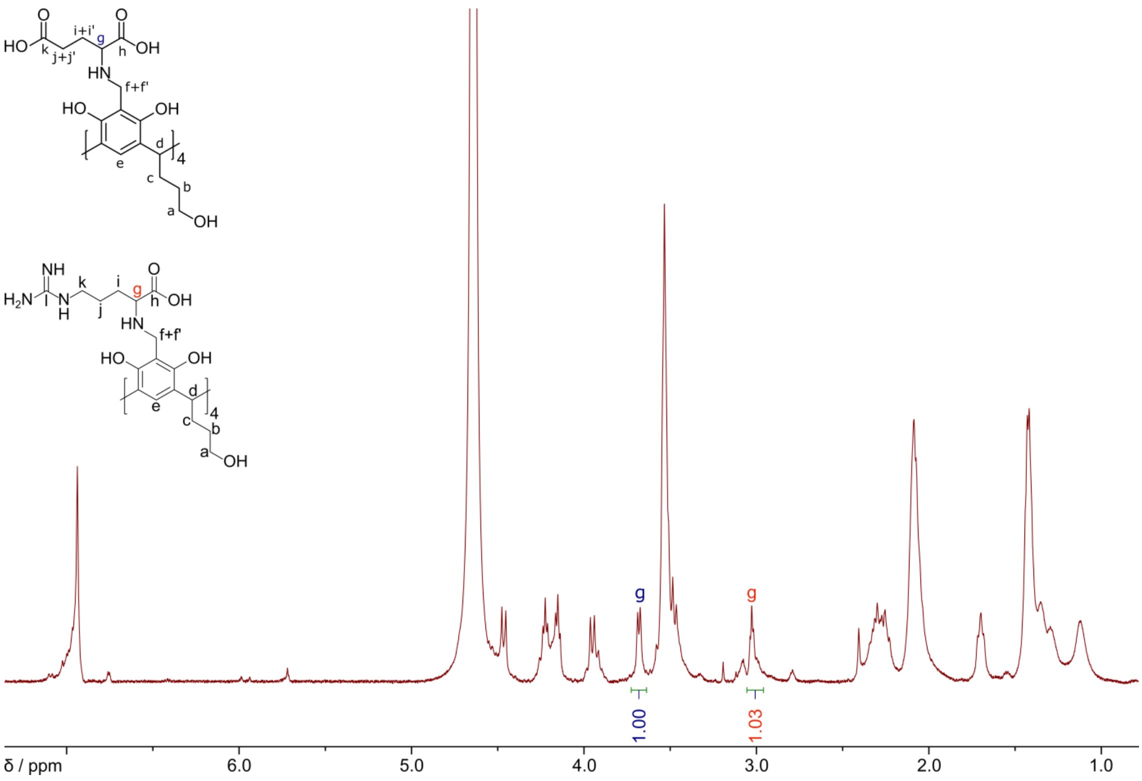

Figure S13. ^{1}H NMR spectrum of D-**GluR**-L-**ArgR** (600 MHz, 298 K, pD 13.0, D_2O, NaOD / DCl).

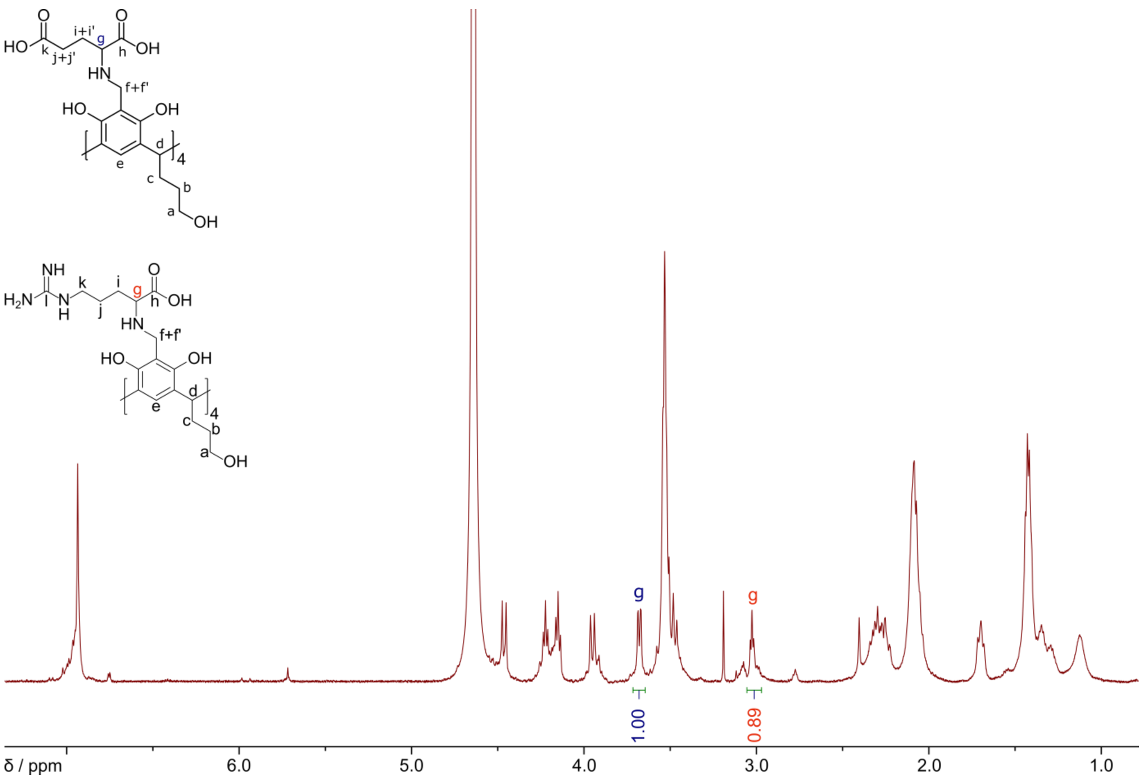

Figure S14. ^{1}H NMR spectrum of L-**GluR**-L-**ArgR** (600 MHz, 298 K, pD 13.0, D_2O, NaOD / DCl).

2.2. DOSY experiments

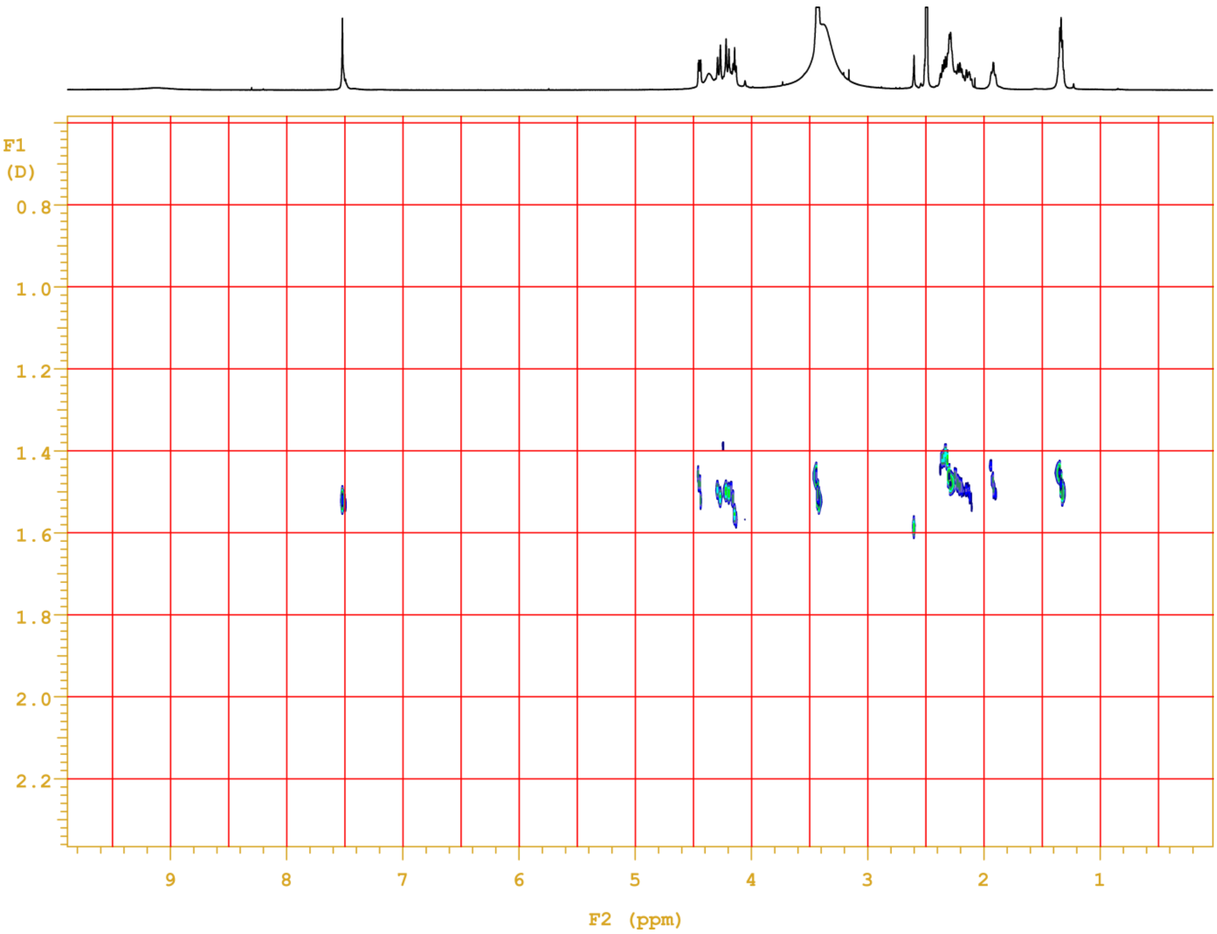

Figure S15. ^{1}H NMR and DOSY spectra of L-**GluR** (C = 20 mM) (600 MHz, 298 K, DMSO).

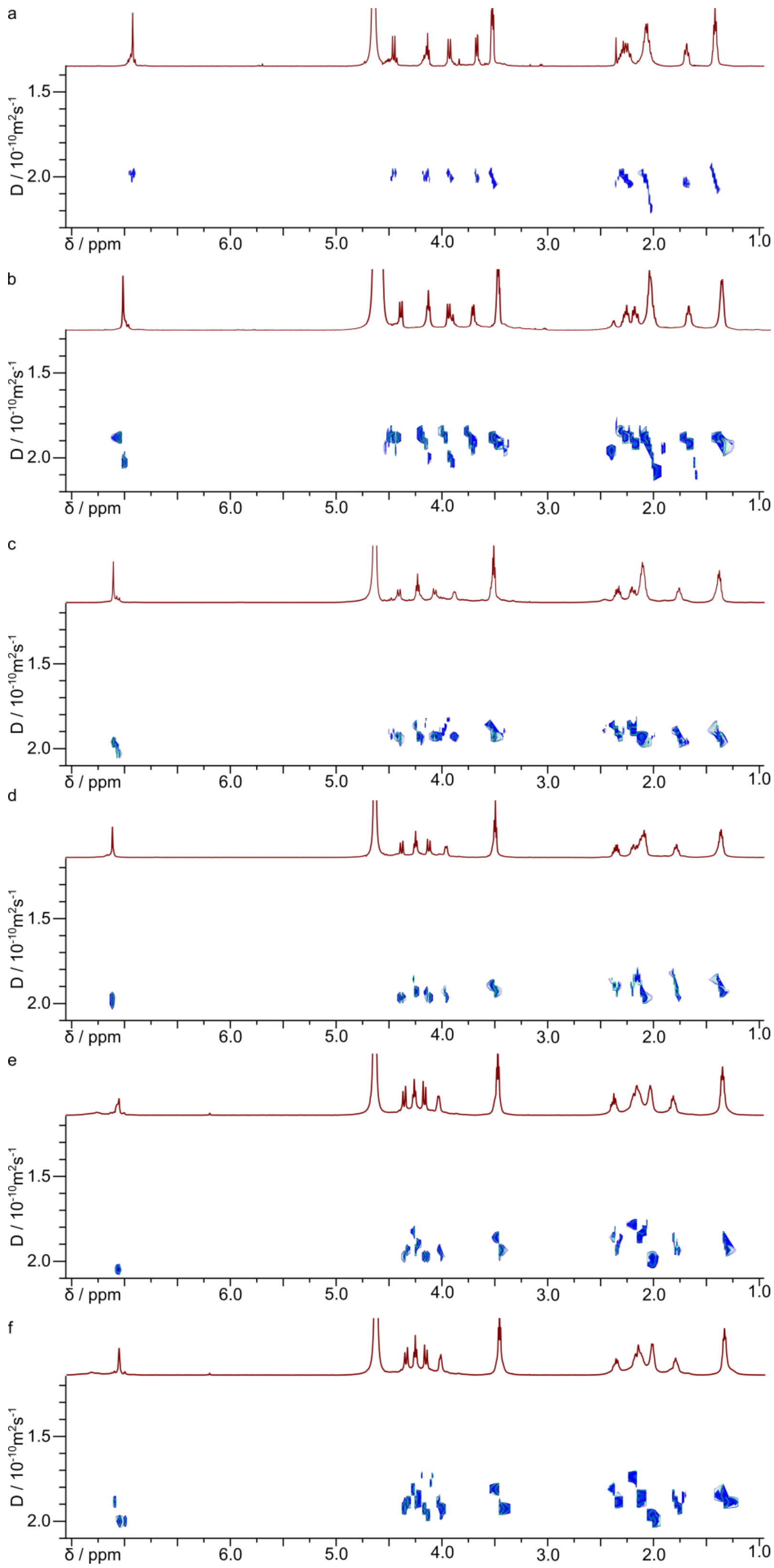

Figure S16. ^{1}H NMR and DOSY spectra of (L-**GluR**)$_2$ (C = 10 mM) at different pD a) 13.3 b) 12.0 c) 10.3 d) 9.0 e) 7.2 f) 5.5 (600 MHz, 298 K, D_2O, NaOD / DCl).

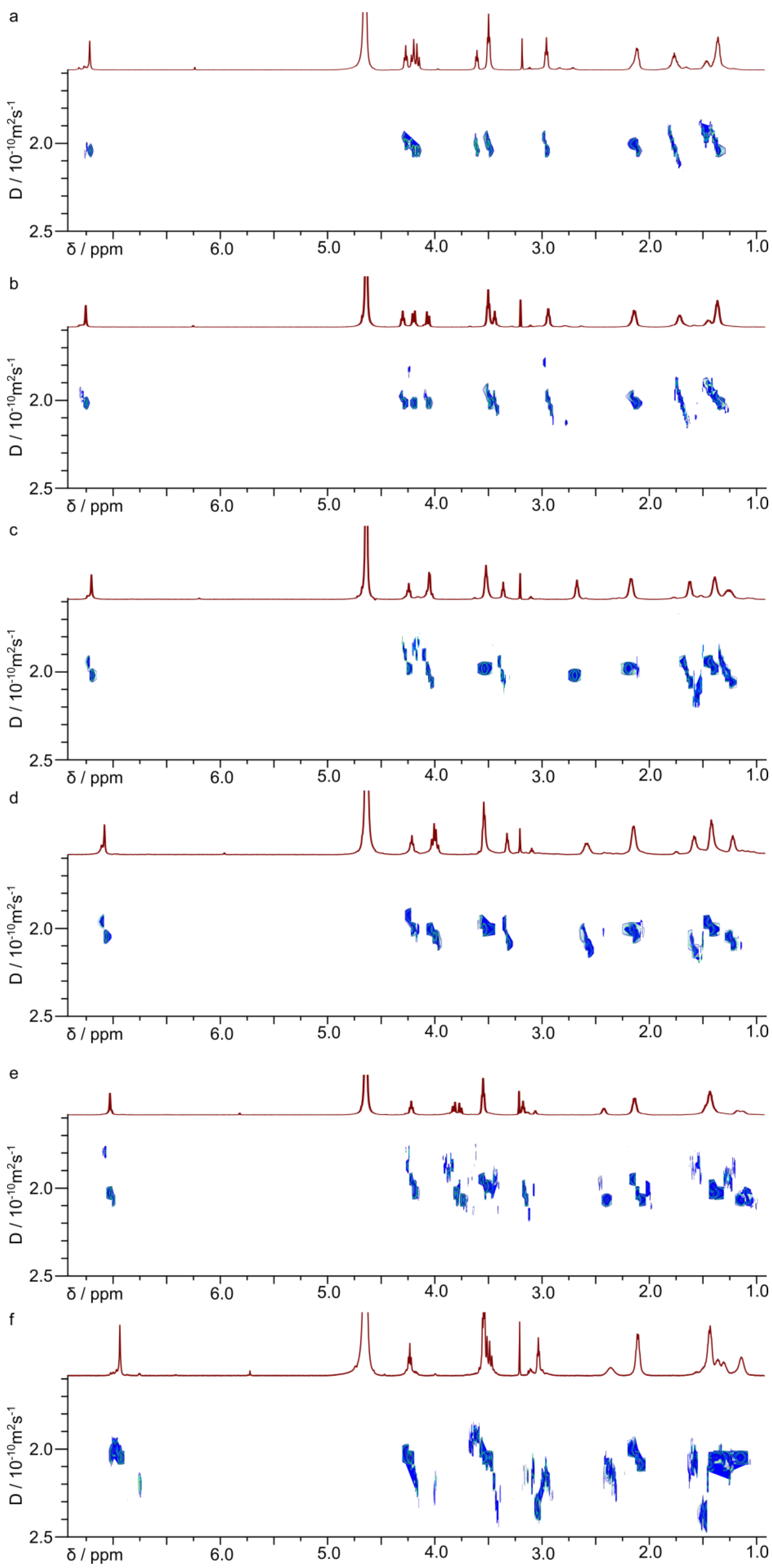

Figure S17. ^{1}H NMR and DOSY spectra of (L-**ArgR**)$_2$ (C = 10 mM) at different pD a) 1.9 b) 5.0 c) 8.0 d) 10.3 e) 12.0 f) 13.3 (600 MHz, 298 K, D_2O, NaOD / DCl).

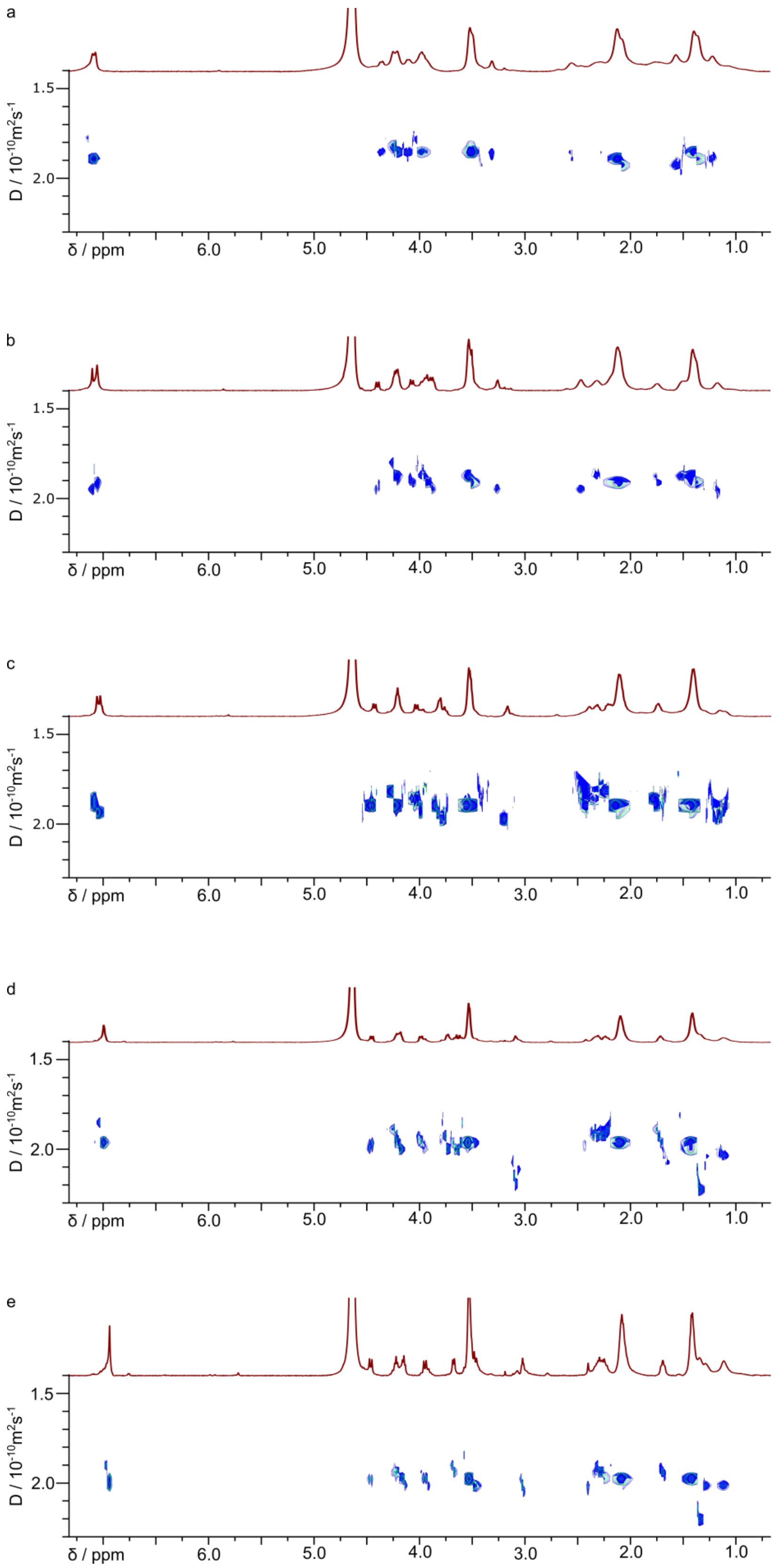

Figure S18. ^{1}H NMR and DOSY spectra of L-**ArgR**-D-**GluR** (C = 10 mM) at different pD a) 9.0 b) 10.0 c) 11.0 d) 12.0 e) 13.0 (600 MHz, 298 K, D_2O, NaOD / DCl).

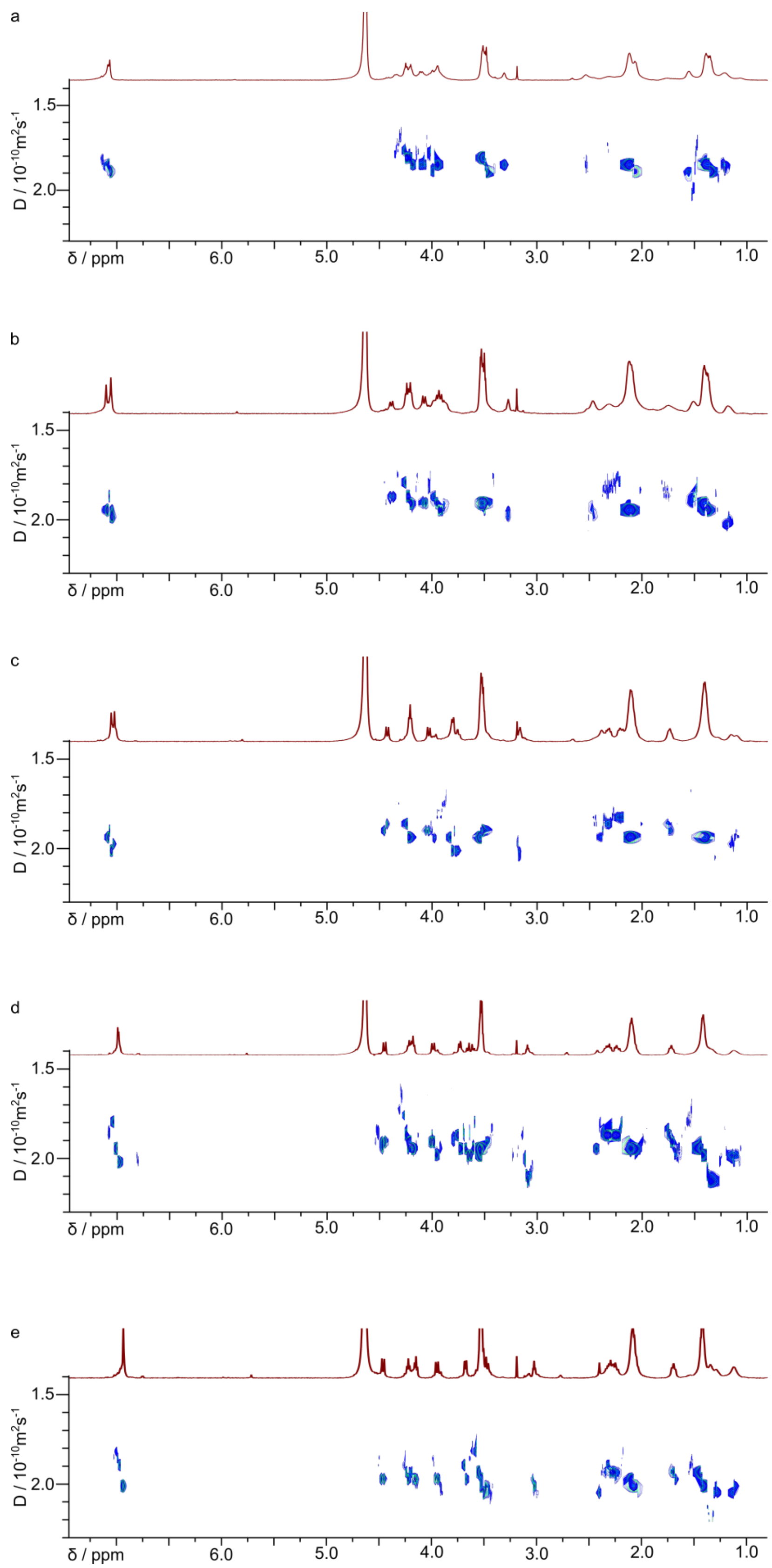

Figure S19. ^{1}H NMR and DOSY spectra of L-**ArgR**-L-**GluR** (C = 10 mM) at different pD a) 9.0 b) 10.0 c) 11.0 d) 12.0 e) 13.0 (600 MHz, 298 K, D_2O, NaOD / DCl).

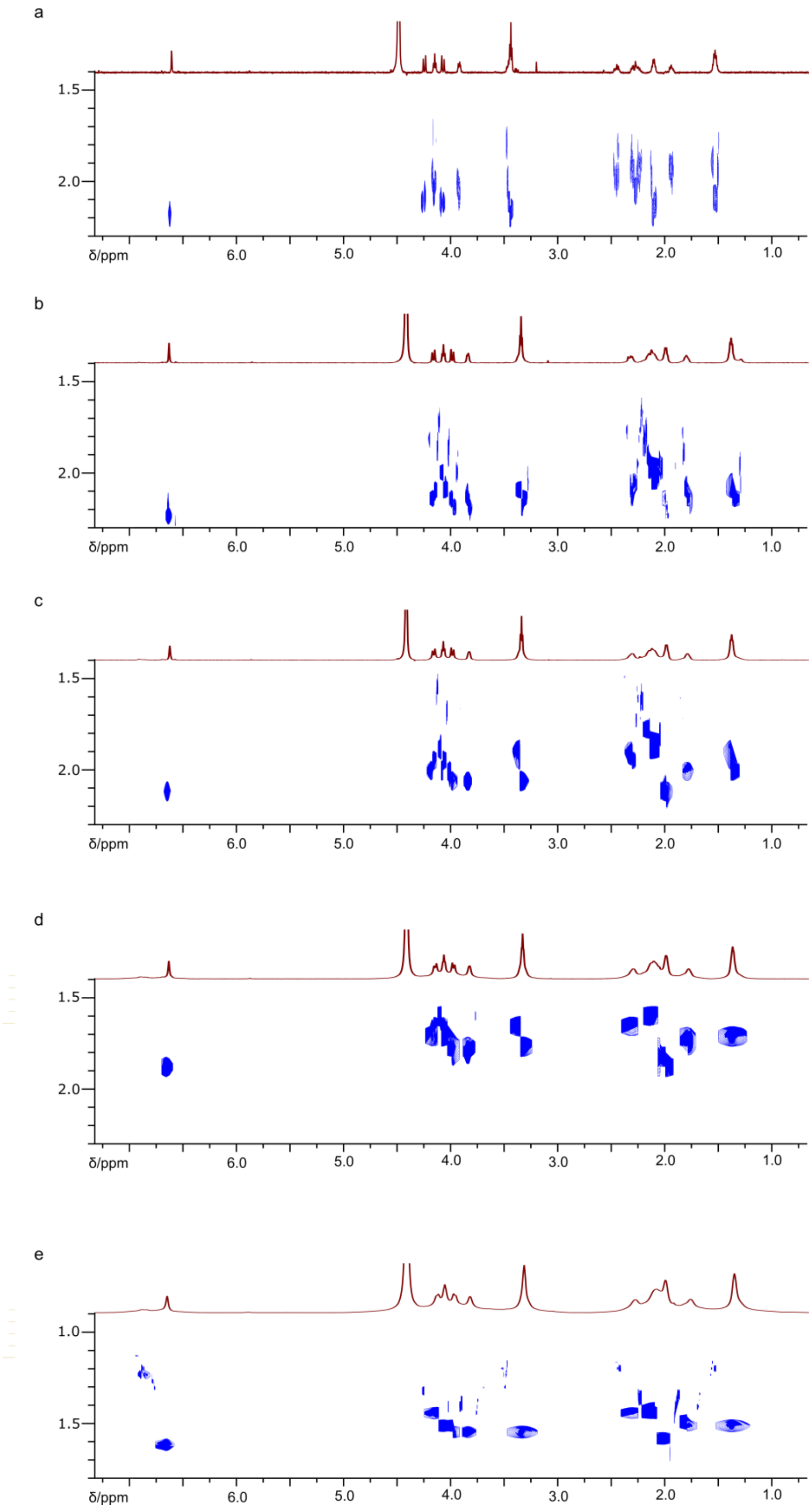

Figure S20. [1]H NMR and DOSY spectra of (L-**GluR**)$_2$ at pD 5.0 at different concentration a) 0.37 mM b) 1.8 mM c) 3.7 mM d) 10 mM e) 14.8 mM (600 MHz, 298 K, D_2O, NaOD / DCl).

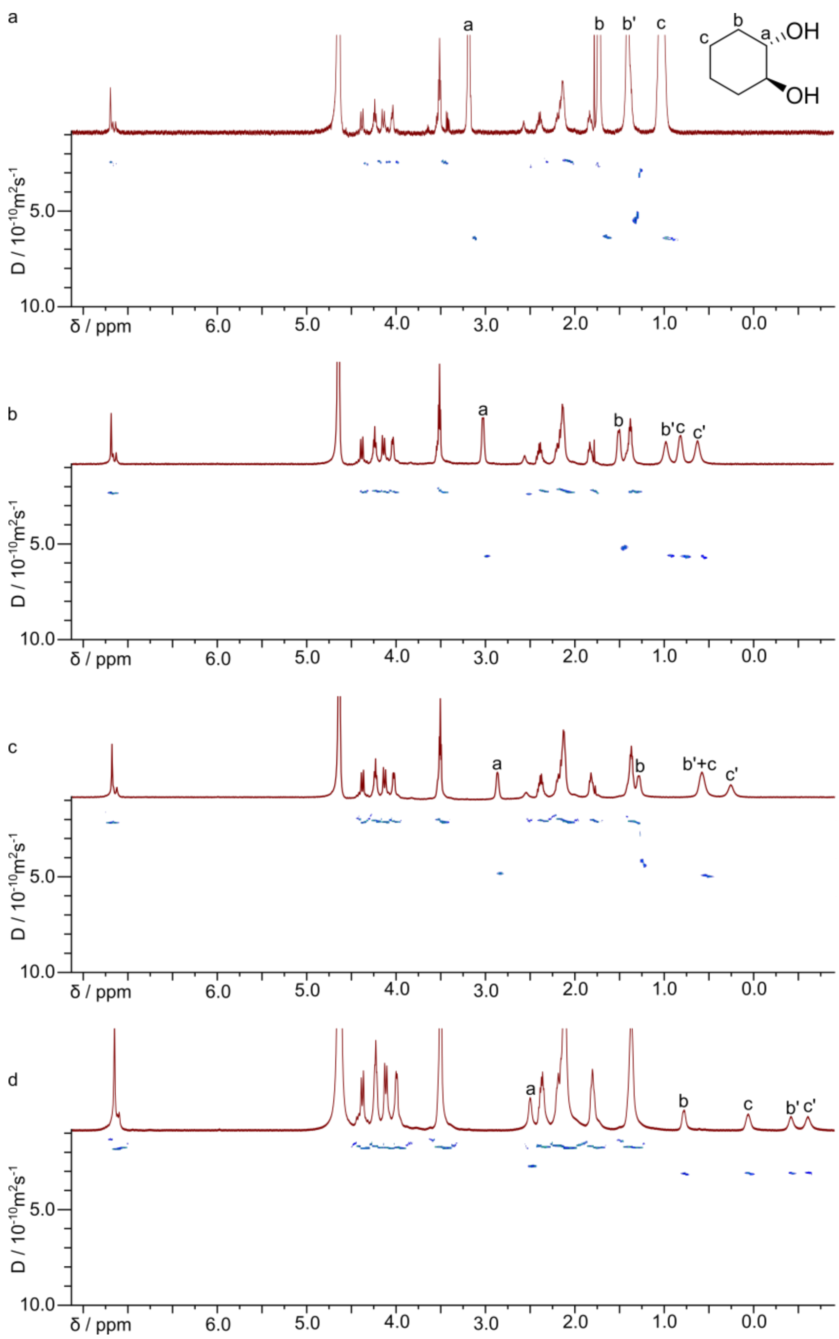

Figure S21. ^{1}H NMR and DOSY spectra for complexation of (1S,2S)-*trans*-1,2-cyclohexanediol **1,** (C = 10 mM) in (L-**GluR**)$_2$ at pD 9.0 at different concentration a) 0.37 mM b) 1.9 mM c) 3.7 mM d) 10 mM (600 MHz, 298 K, D_2O, NaOD / DCl).

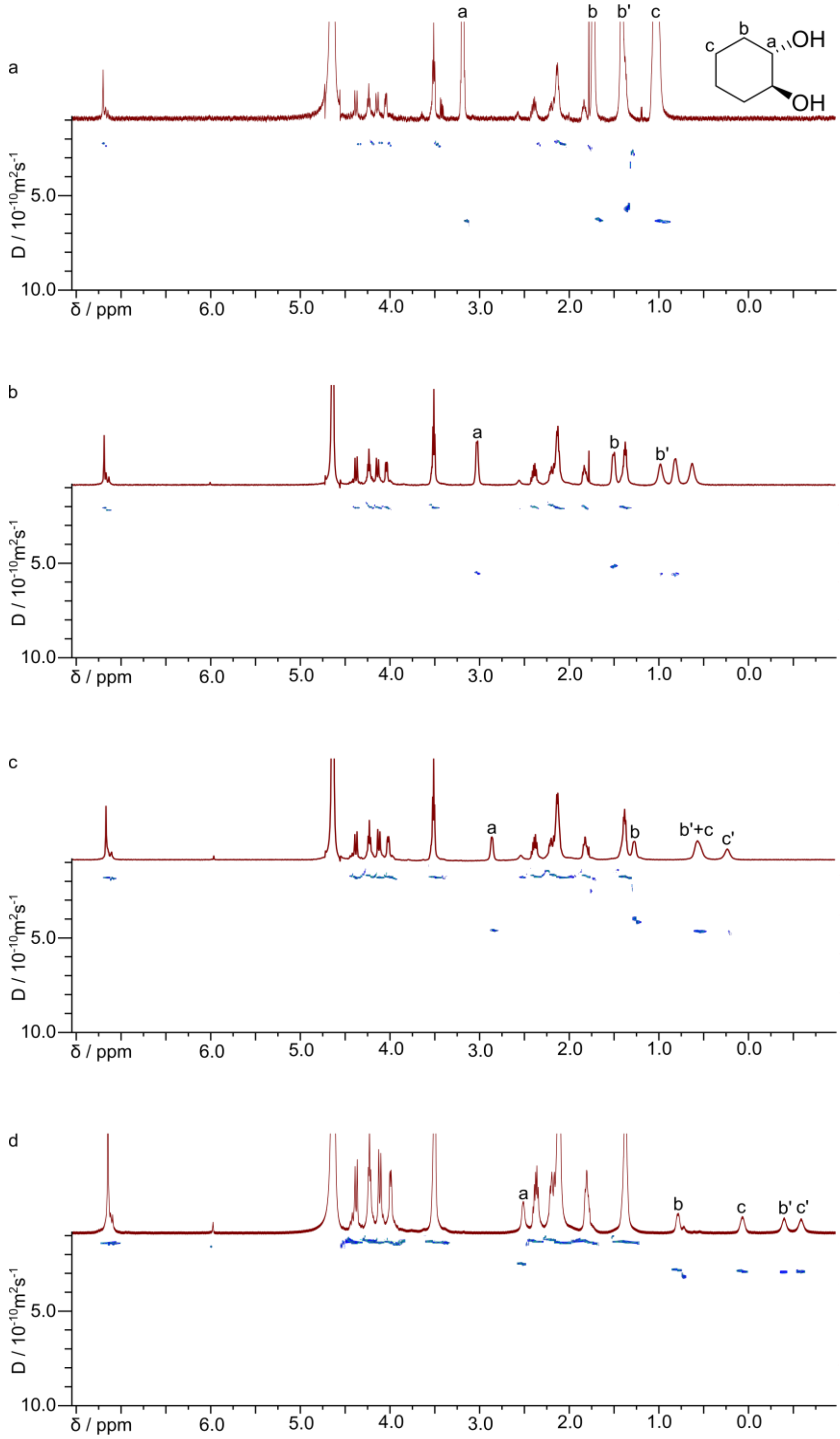

Figure S22. [1]H NMR and DOSY spectra for complexation of (1S,2S)-*trans*-1,2-cyclohexanediol **1**, (C = 10 mM) in (D-**GluR**)$_2$ at pD 9.0 at different concentration in a) 0.37 mM b) 1.9 mM c) 3.7 mM d) 10 mM (600 MHz, 298 K, D_2O, NaOD / DCl).

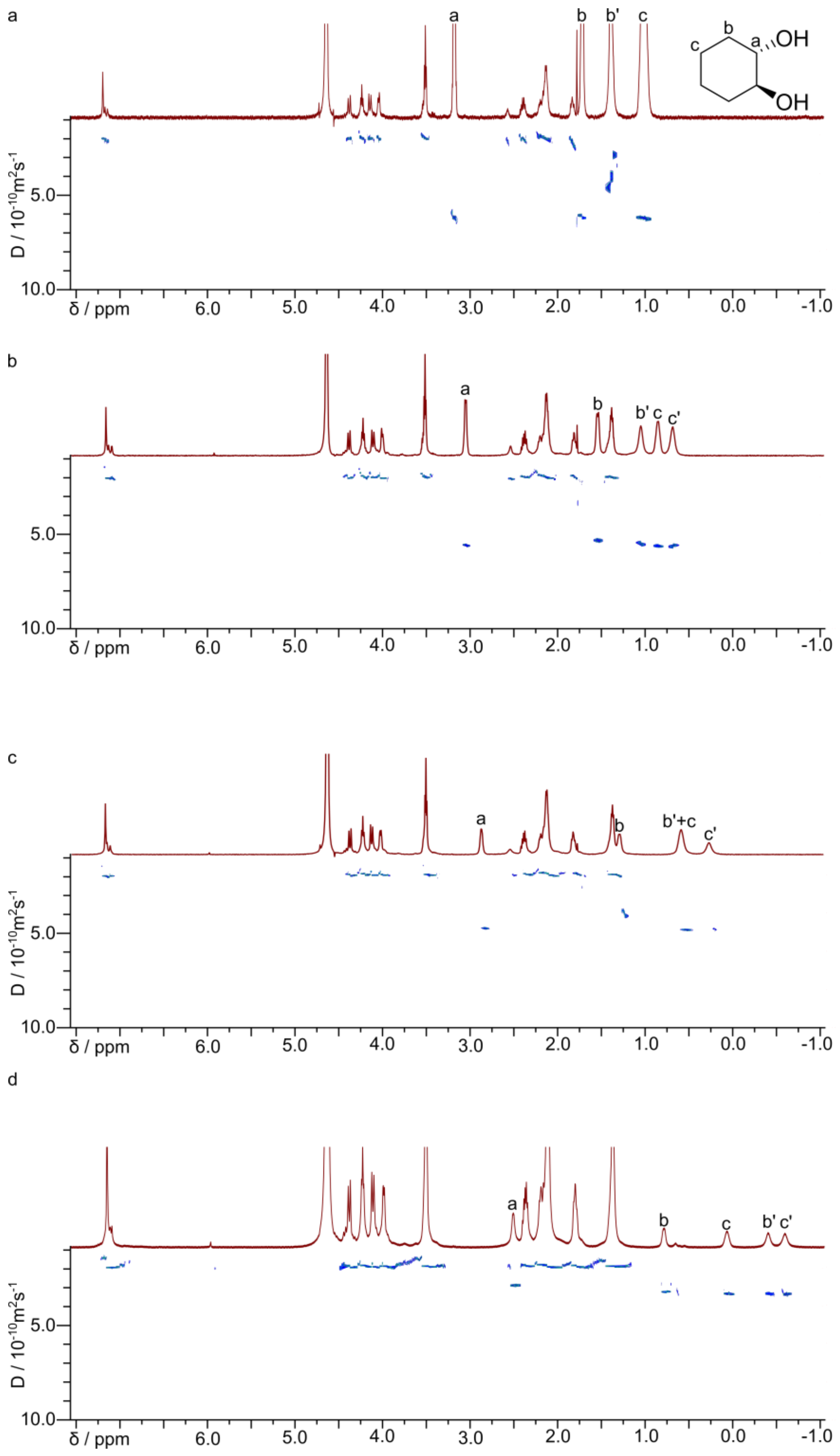

Figure S23. ^{1}H NMR and DOSY spectra for complexation of (1S,2S)-*trans*-1,2-cyclohexanediol **1**, (C = 10 mM) in D-**GluR**-L-**GluR** at pD 9.0 at different concentration a) 0.37 mM b) 1.9 mM c) 3.7 mM d) 10 mM (600 MHz, 298 K, D_2O, NaOD / DCl).

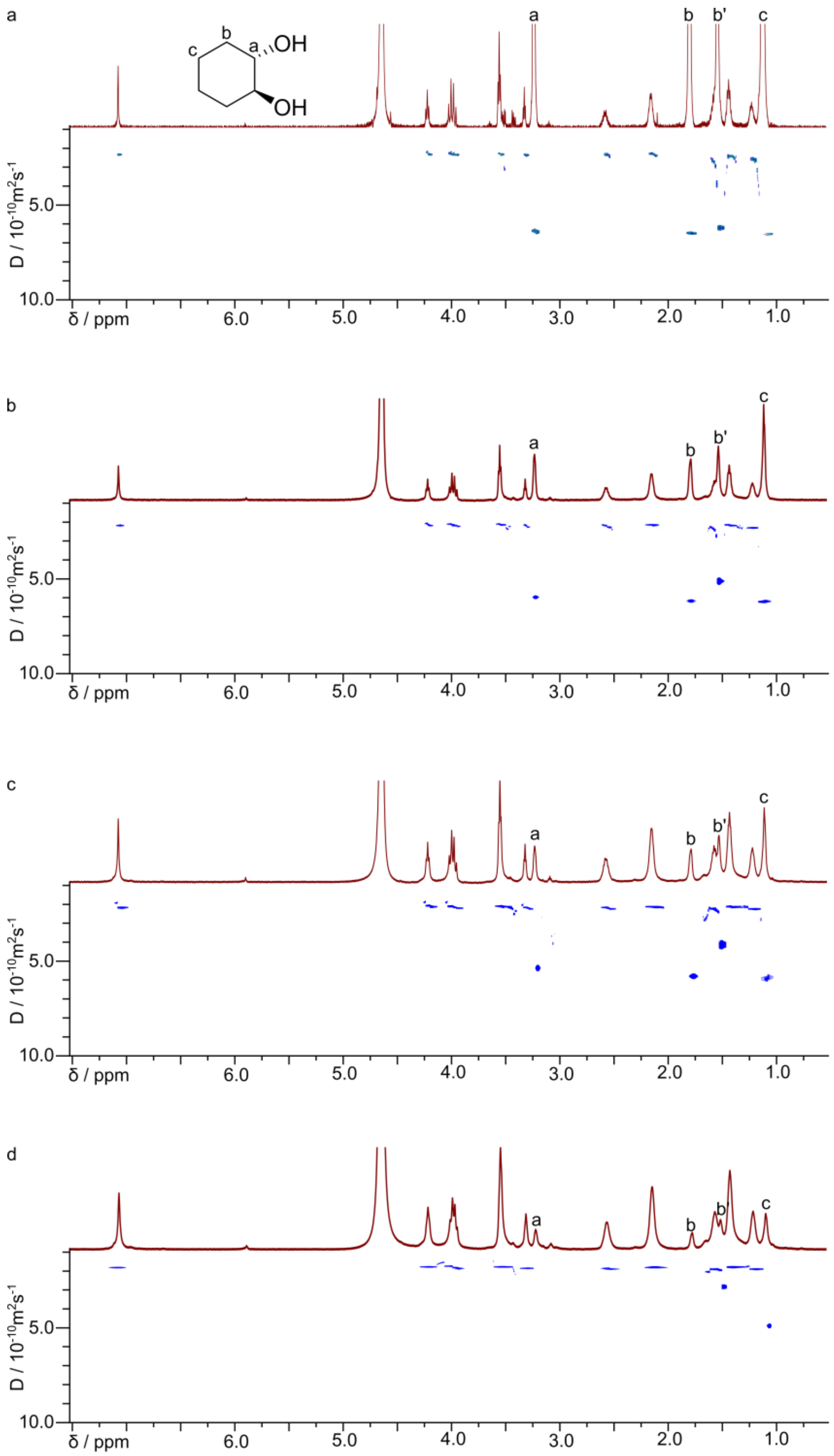

Figure S24. ^{1}H NMR and DOSY spectra for complexation of (1S,2S)-*trans*-1,2-cyclohexanediol **1**, (C = 10 mM) in (L-**ArgR**)$_2$ at pD 9.0 at different concentration a) 0.37 mM b) 1.9 mM c) 3.7 mM d) 10 mM (600 MHz, 298 K, D_2O, NaOD / DCl).

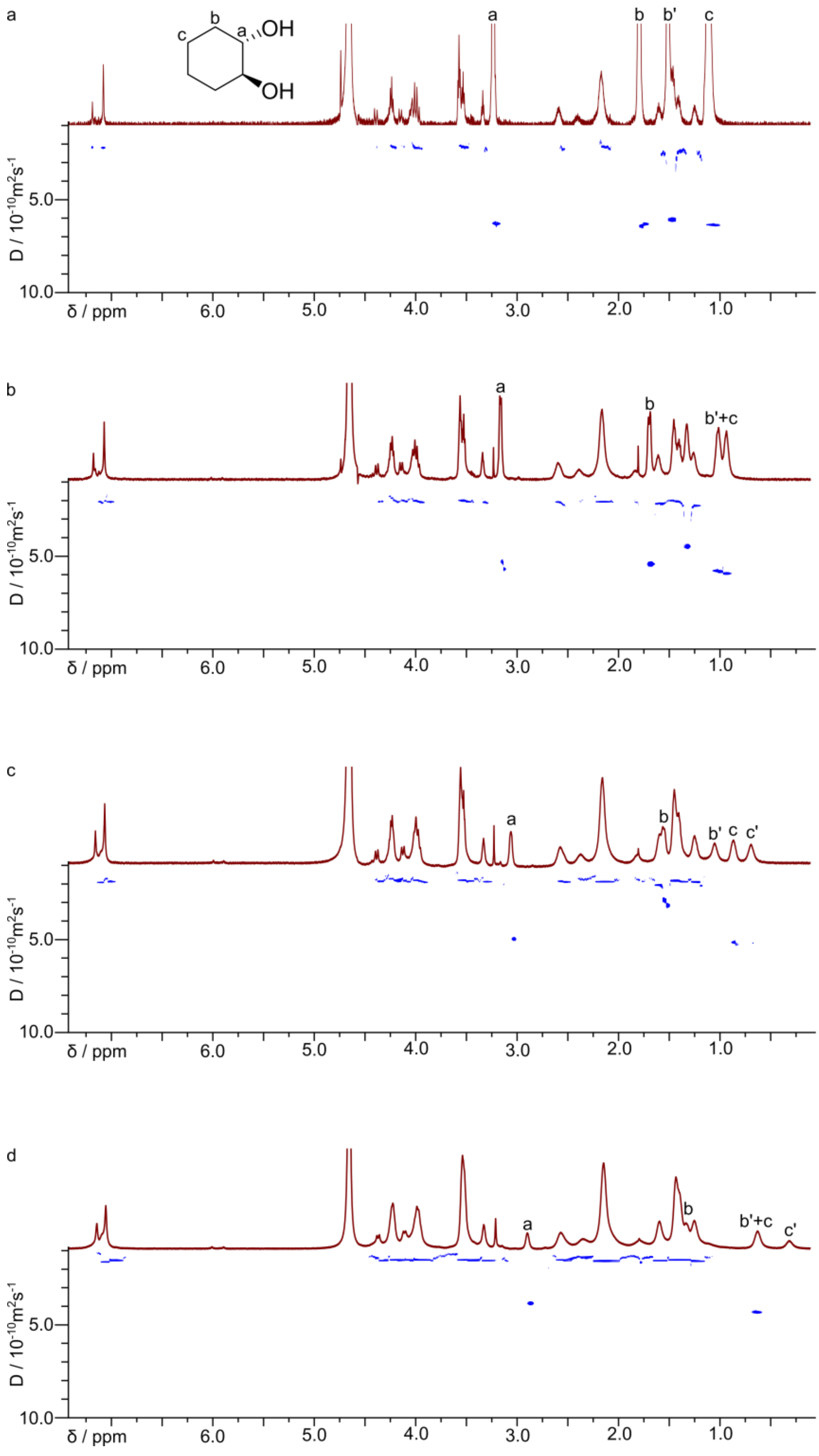

Figure S25. ^{1}H NMR and DOSY spectra for complexation of (1S,2S)-*trans*-1,2-cyclohexanediol **1,** (C = 10 mM) in D-**GluR**-L-**ArgR** at pD 9.0 at different concentration a) 0.37 mM b) 1.9 mM c) 3.7 mM d) 10 mM (600 MHz, 298 K, D_2O, NaOD / DCl).

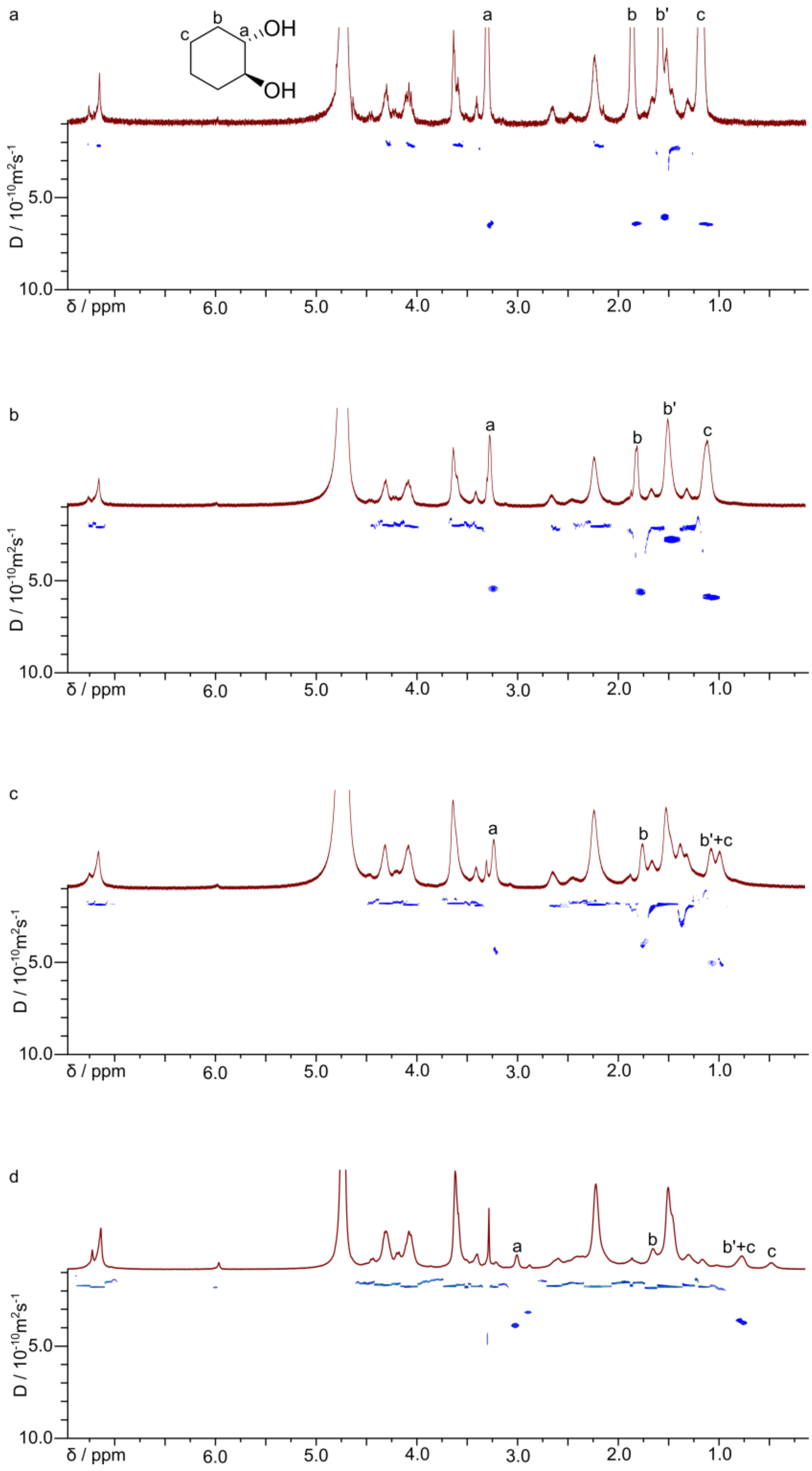

Figure S26. ^{1}H NMR and DOSY spectra for complexation of (1S,2S)-*trans*-1,2-cyclohexanediol **1**, (C = 10 mM) in L-**GluR**-L-**ArgR** at pD 9.0 at different concentration a) 0.37 mM b) 1.9 mM c) 3.7 mM d) 10 mM (600 MHz, 298 K, D_2O, NaOD / DCl).

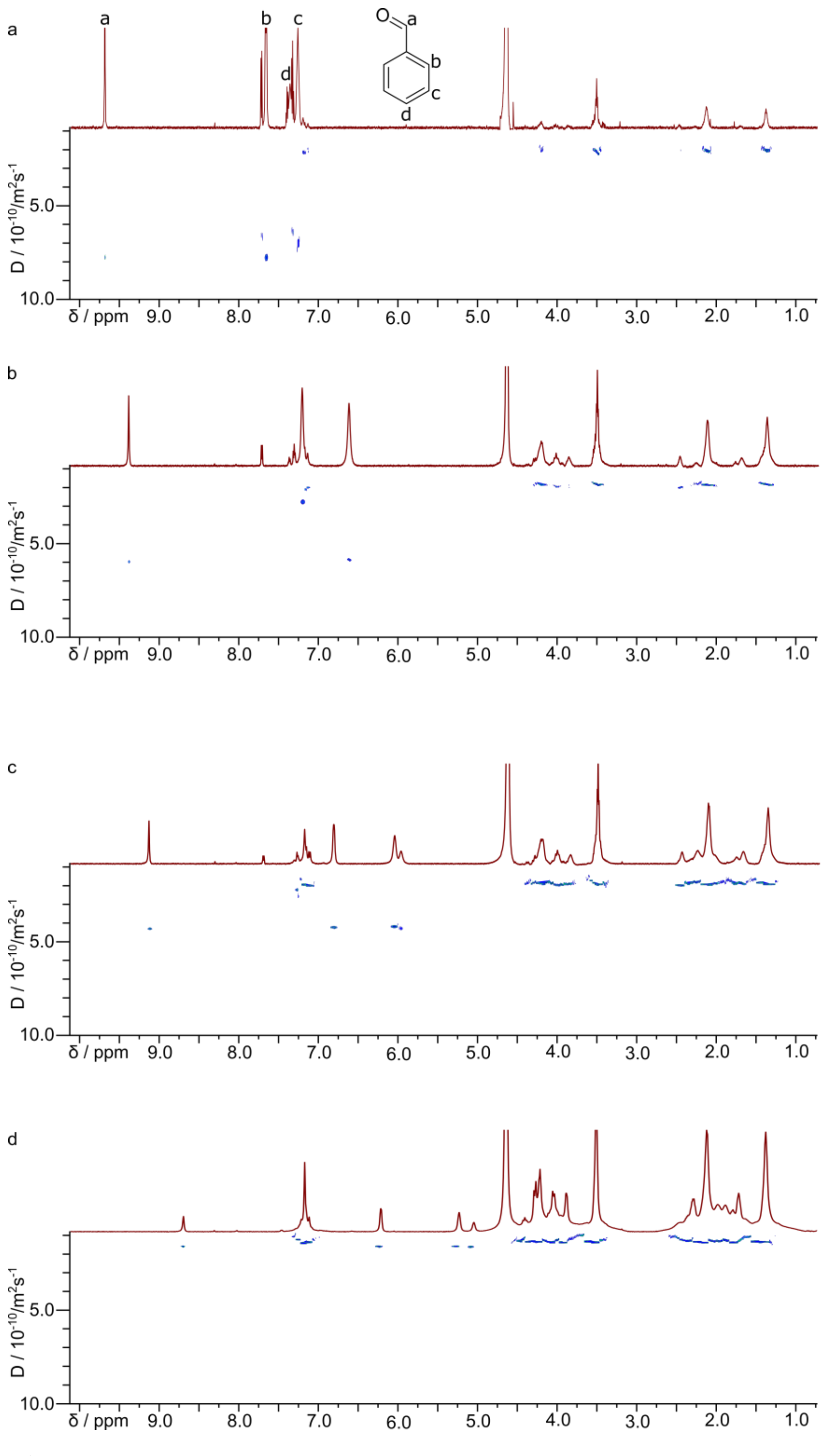

Figure S27. ^{1}H NMR and DOSY spectra for complexation of benzaldehyde **2** (saturation) in D_2O at pD 9.0 at different concentrations of (L-**GluR**)$_2$: a) 0.37 mM (integral-based ratio **2** : (L-**GluR**)$_2$ 1 : 0.05); b) 1.9 mM (integral-based ratio **2** : (L-**GluR**)$_2$ 1 : 0.1); c) 3.7 mM (integral-based ratio **2** : (L-**GluR**)$_2$ 1 : 0.2); d) 10.0 mM (integral-based ratio **2** : (L-**GluR**)$_2$ 1 : 0.6) (600 MHz, 298 K, D_2O, NaOD / DCl).

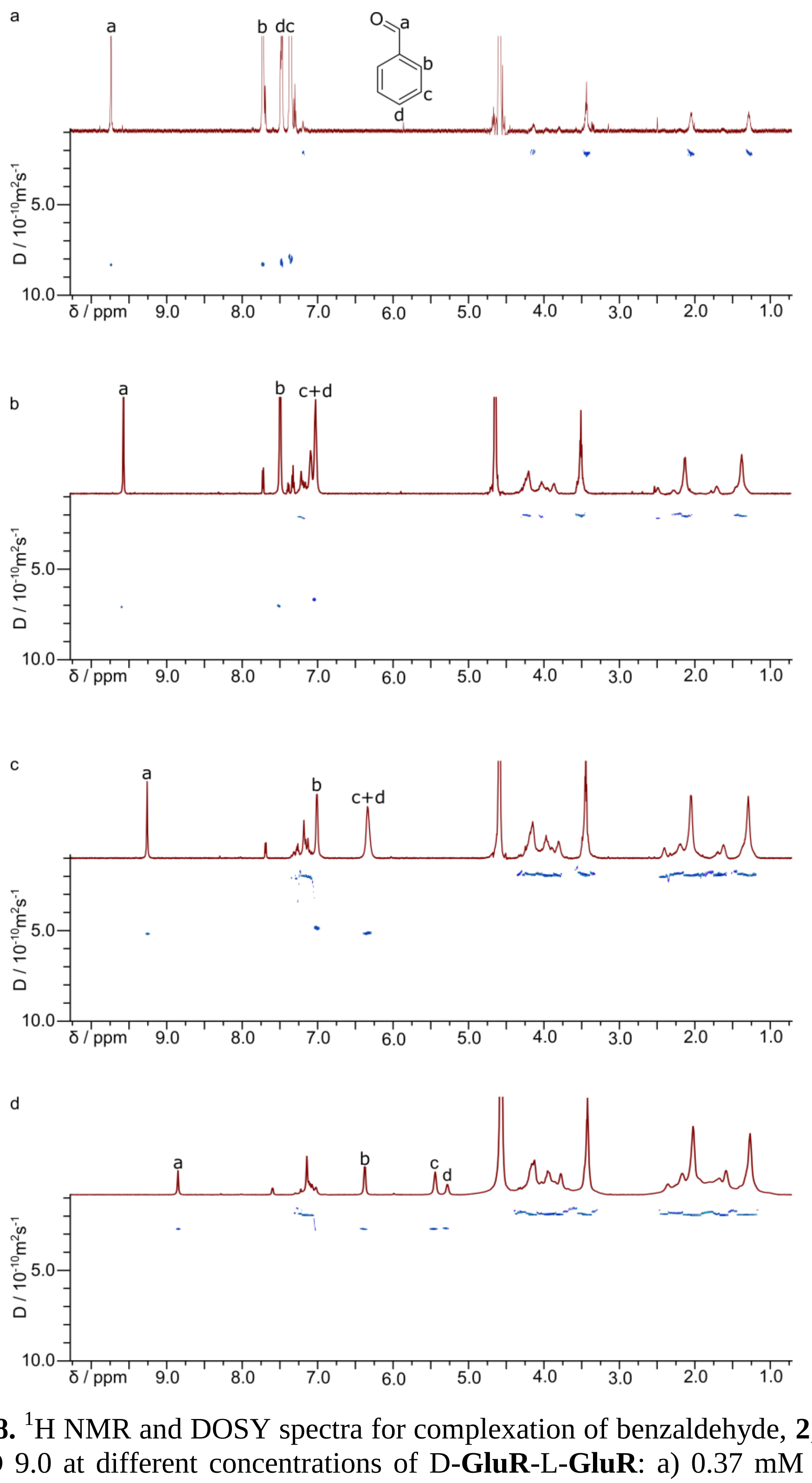

Figure S28. [1]H NMR and DOSY spectra for complexation of benzaldehyde, **2**, (saturation) in D_2O at pD 9.0 at different concentrations of D-**GluR**-L-**GluR**: a) 0.37 mM (integral-based ratio **2** : D-**GluR**-L-**GluR** 1 : 0.03); b) 1.9 mM (integral-based ratio **2** : D-**GluR**-L-**GluR** 1 : 0.1); c) 3.7 mM (integral-based ratio **2** : D-**GluR**-L-**GluR** 1 : 0.3); d) 10.0 mM (integral-based ratio **2** : D-**GluR**-L-**GluR** 1 : 0.6) (600 MHz, 298 K, D_2O, NaOD / DCl).

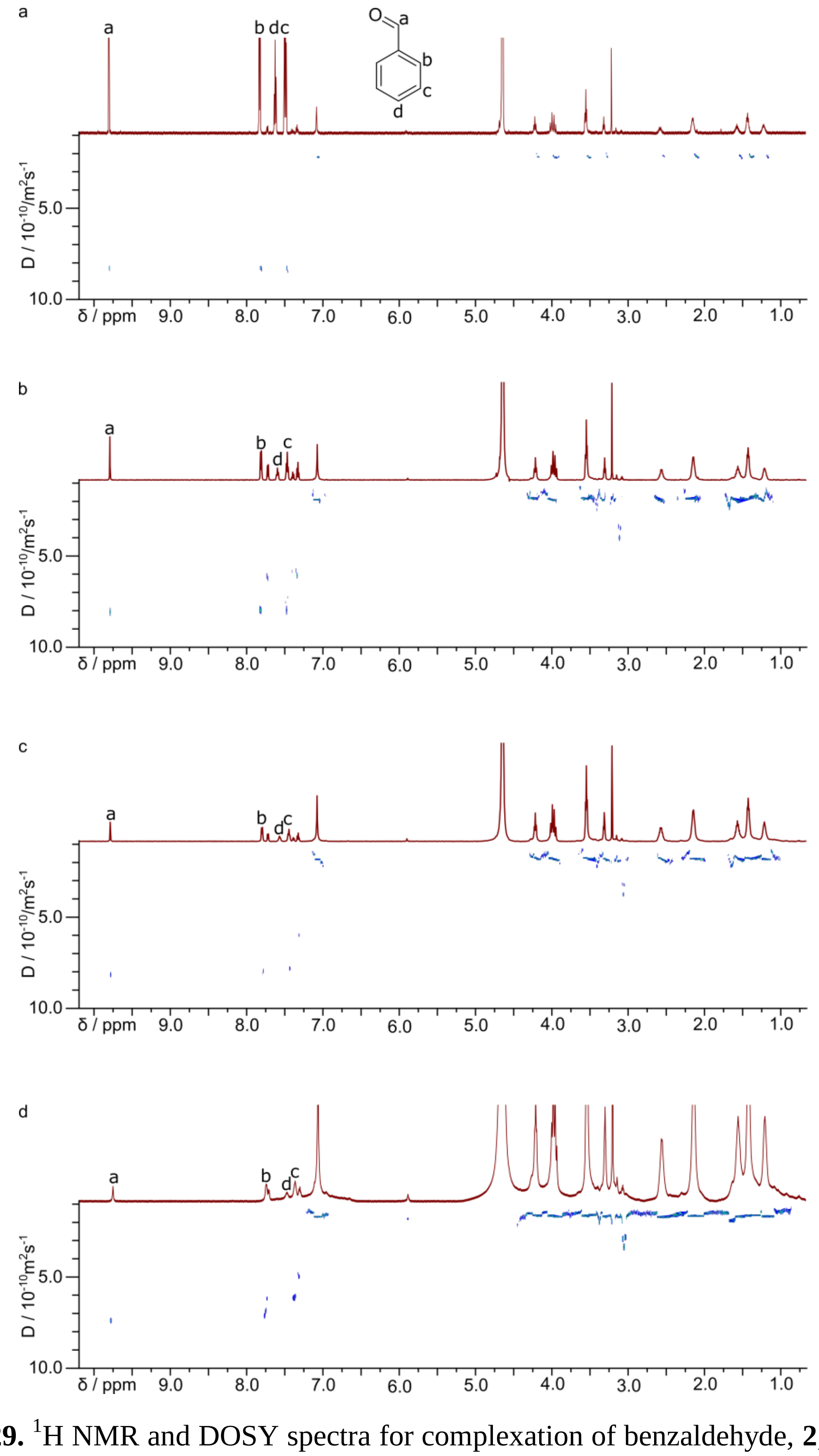

Figure S29. [1]H NMR and DOSY spectra for complexation of benzaldehyde, **2**, (saturation) in D_2O at pD 9.0 at different concentrations of (L-**ArgR**)$_2$: a) 0.33 mM (integral-based ratio **2** : (L-**ArgR**)$_2$ 1 : 0.04); b) 1.6 mM (integral-based ratio **2** : (L-**ArgR**)$_2$ 1 : 0.4); c) 3.3 mM (integral-based ratio **2 0** : (L-**ArgR**)$_2$ 1 : 0.7); d) 9.0 mM (integral-based ratio **2** : (L-**ArgR**)$_2$ 1 : 2.0) (600 MHz, 298 K, D_2O, NaOD / DCl).

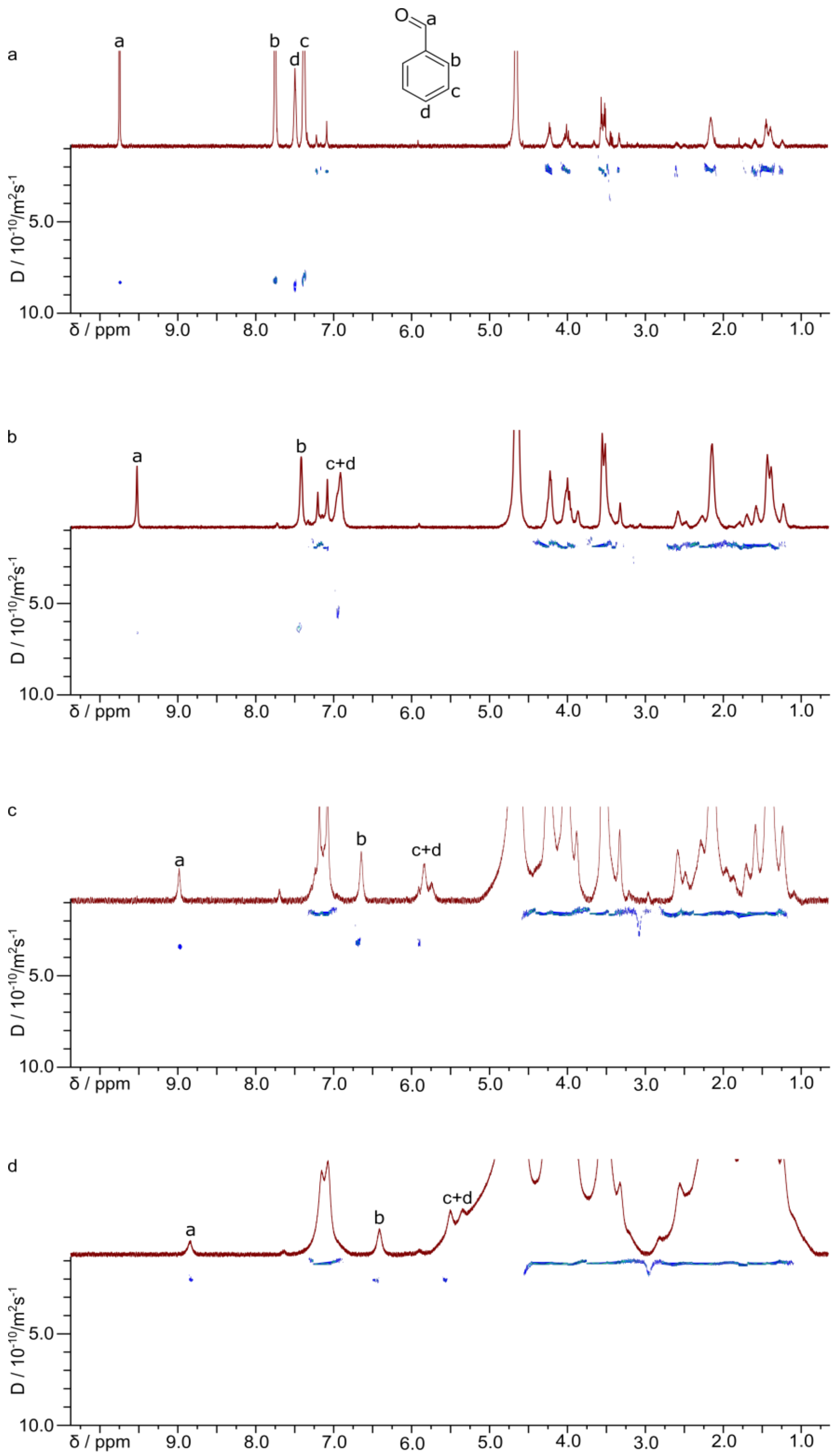

Figure S30. [1]H NMR and DOSY spectra for complexation of benzaldehyde **2** (saturation) in D_2O at pD 9.0 at different concentrations of D-**GluR**-L-**ArgR**: a) 0.35 mM (integral-based ratio **2** : D-**GluR**-L-**ArgR** 1:0.04); b) 1.7 mM (integral-based ratio **2** : D-**GluR**-L-**ArgR** 1 : 0.3); c) 3.5 mM (integral-based ratio **2** : L-**ArgR**-D-**GluR** 1 : 1.4); d) 9.6 mM (integral-based ratio **2** : D-**GluR**-L-**ArgR** 1 : 2.5) (600 MHz, 298 K, D_2O, NaOD / DCl).

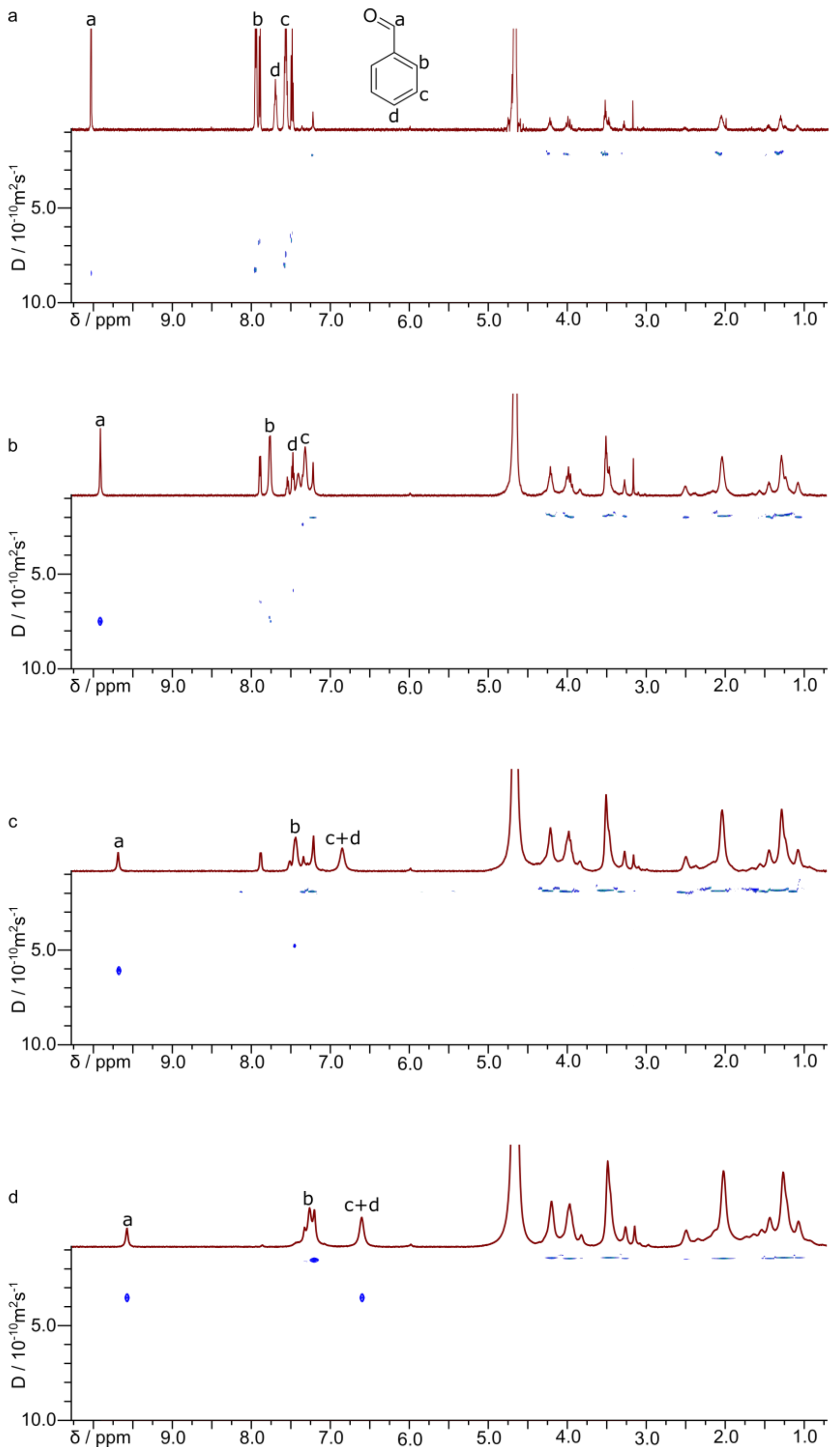

Figure S31. [1]H NMR and DOSY spectra for complexation of benzaldehyde, **2**, (saturation) in D_2O at pD 9.0 at different concentrations of L-**GluR**-L-**ArgR**: a) 0.35 mM (integral-based ratio **2** : L-**ArgR**-L-**GluR** 1 : 0.04); b) 1.8 mM (integral-based ratio **2** : L-**GluR**-L-**ArgR** 1 : 0.2); c) 3.5 mM (integral-based ratio **2** : L-**GluR**-L-**ArgR** 1 : 0.5); d) 9.5 mM (integral-based ratio **2** : L-**GluR**-L-**ArgR** 1 : 1.1) (600 MHz, 298 K, D_2O, NaOD / DCl).

2.3. Complexation of guests

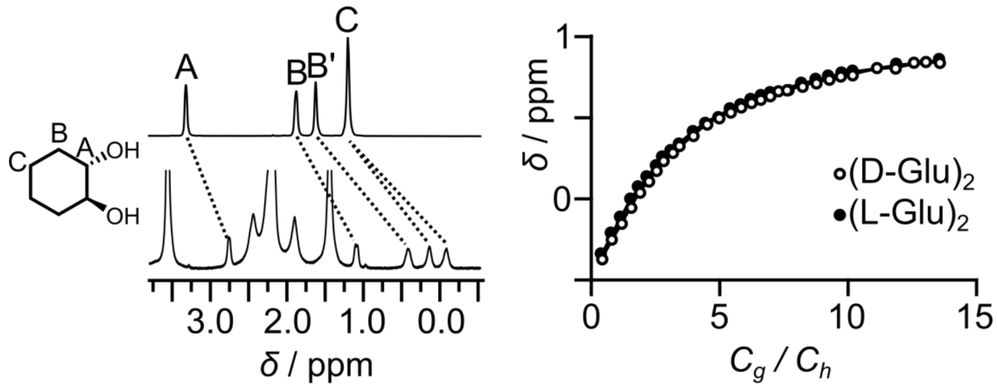

$$(\mathbf{GluR})_2 + \mathbf{1} \xrightleftharpoons{K_1} (\mathbf{GluR})_2\mathbf{1}$$

$$(\mathbf{GluR})_2\mathbf{1} + \mathbf{1} \xrightleftharpoons{K_2} (\mathbf{GluR})_2(\mathbf{1})_2$$

	K_1	σ_1	K_2	σ_2
(D-**GluR**)$_2$+**1**	4.84	0.03	1.85	0.03
(L-**GluR**)$_2$+**1**	4.81	0.04	1.73	0.03

Figure S32. ^{1}H NMR spectra for complexation of (1S,2S)-*trans*-1,2-cyclohexanediol **1** in (**GluR**)$_2$ (1 : 1 guest : host ratio) and the titration curves (400 MHz, 303 K, pD 4.8, D_2O, NaOD / DCl).

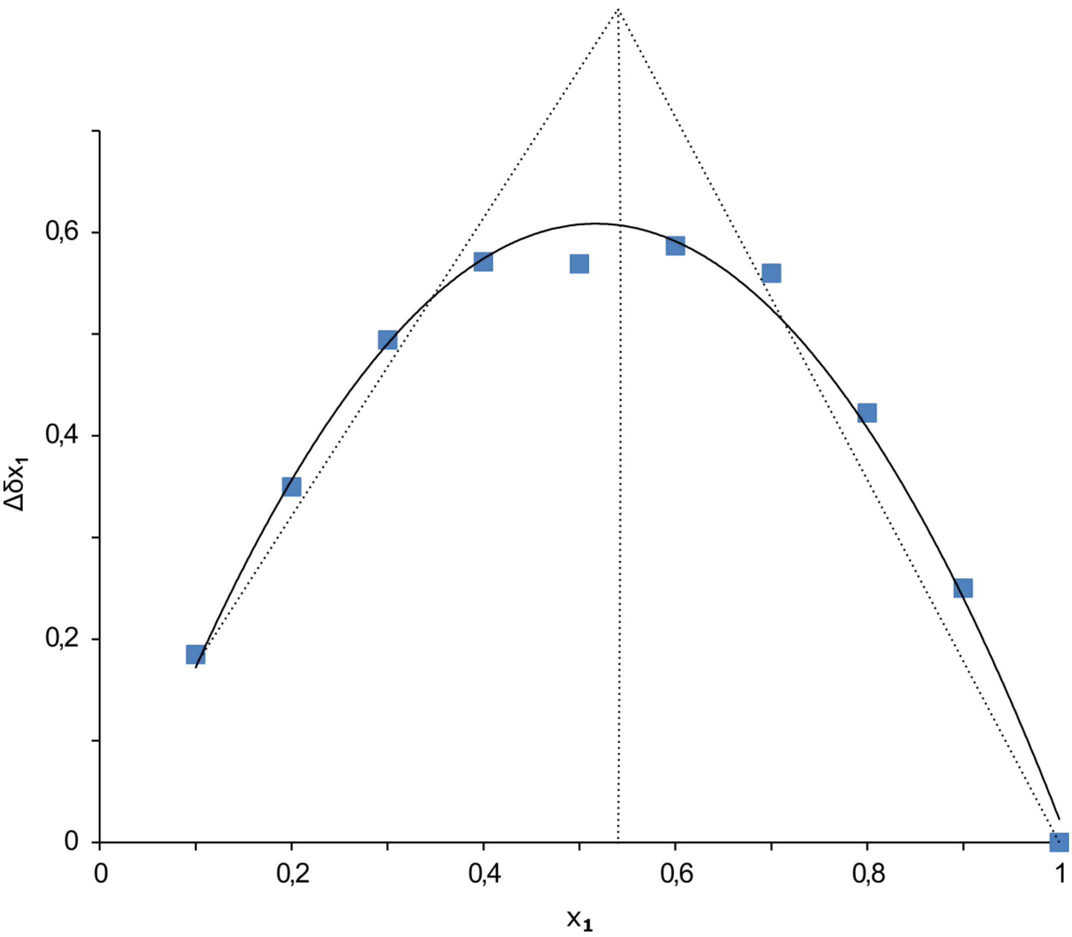

Figure S33. Job plot of (L-**GluR**)$_2$ and **1** (400 MHz, 303 K, pD 4.8, D_2O, NaOD / DCl).

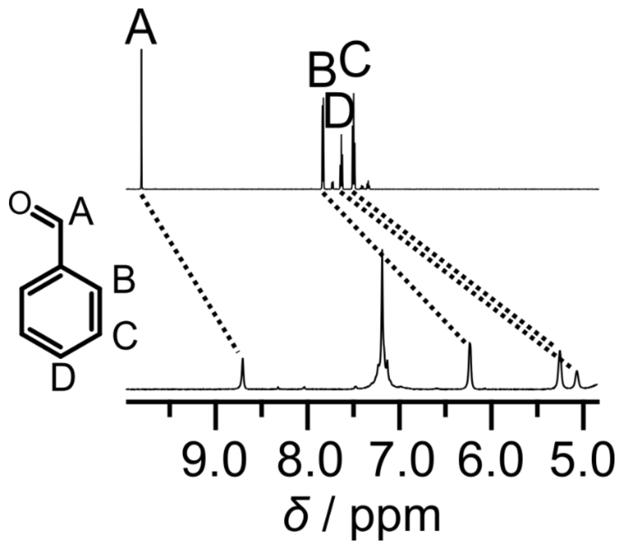

Figure S34. ^{1}H NMR spectra for complexation of benzaldehyde **2** in (L-**GluR**)$_2$ (1 : 1 guest : host ratio, 400 MHz, 303 K, pD 4.8, D_2O, NaOD / DCl).

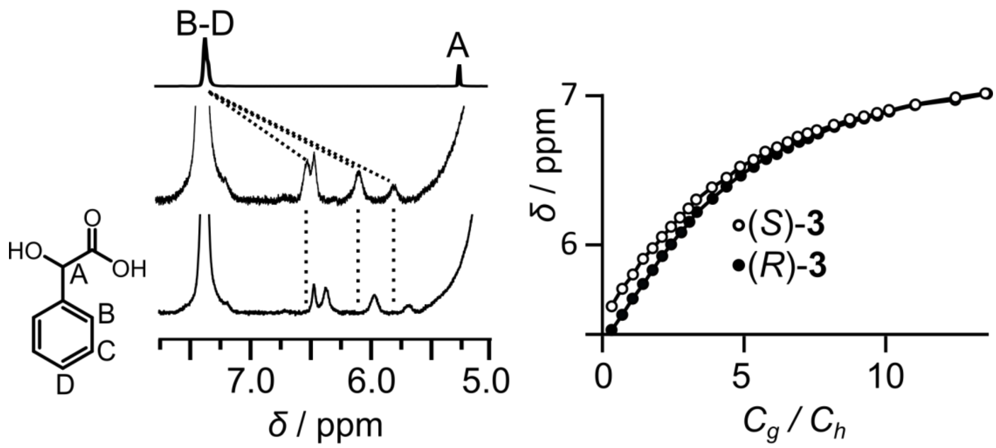

$$(\text{L-}\mathbf{ArgR})_2 + \mathbf{3} \overset{K_1}{\rightleftharpoons} (\text{L-}\mathbf{ArgR})_2\mathbf{3}$$

$$(\text{L-}\mathbf{ArgR})_2\mathbf{3} + \mathbf{3} \overset{K_2}{\rightleftharpoons} (\text{L-}\mathbf{ArgR})_2(\mathbf{3})_2$$

	K_1	σ_1	K_2	σ_2
(L-**ArgR**)+(*R*)-**3**	4.78	0.02	1.85	0.02
(L-**ArgR**)+(*S*)-**3**	4.34	0.03	1.77	0.03

Figure S35. [1]H NMR spectra for complexation of mandelic acid **3** in (L-**ArgR**)$_2$ (1 : 1 guest : host ratio, (*S*)-**3** middle, (*R*)-**3** bottom) and the titration curves (400 MHz, 303 K, pD 4.8, D_2O, NaOD / DCl).

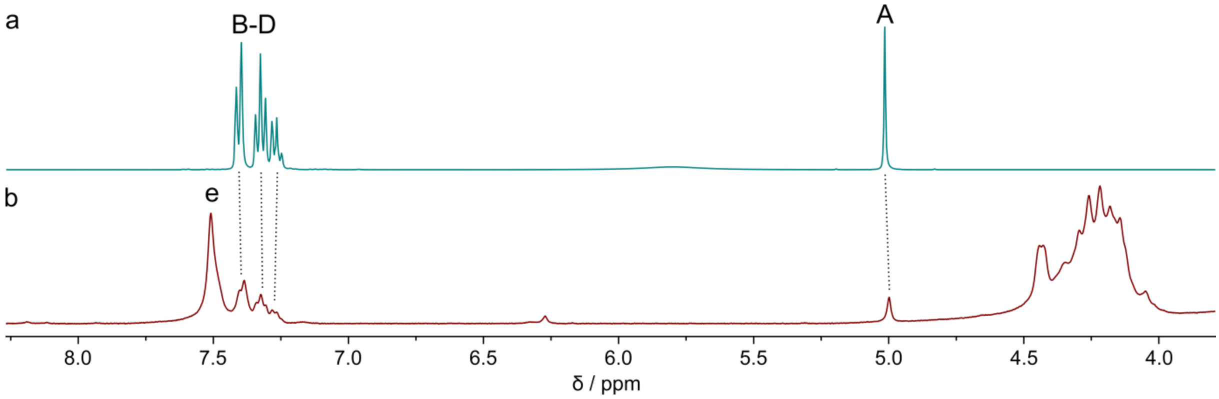

Figure S36. [1]H NMR spectra of a) mandelic acid **3** b) mandelic acid **3** in L-**GluR** (1 : 1 guest : host ratio) (400 MHz, 303 K, DMSO).

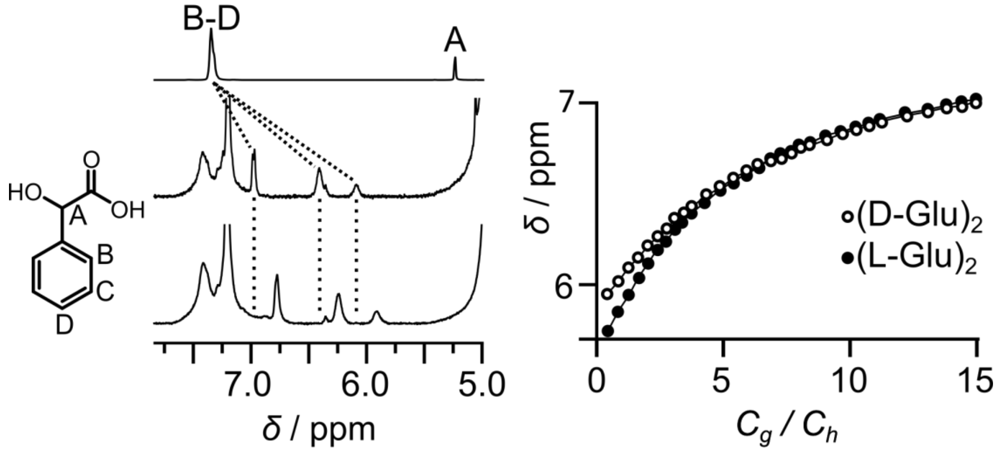

$$(\mathbf{GluR})_2 + \mathbf{3} \underset{}{\overset{K_1}{\rightleftharpoons}} (\mathbf{GluR})_2\mathbf{3}$$

$$(\mathbf{GluR})_2\mathbf{3} + \mathbf{3} \underset{}{\overset{K_2}{\rightleftharpoons}} (\mathbf{GluR})_2(\mathbf{3})_2$$

	K_1	σ_1	K_2	σ_2
(D-**GluR**)$_2$+(*R*)-**3**	4.85	0.02	1.25	0.02
(L-**GluR**)$_2$+(*R*)-**3**	4.20	0.03	1.80	0.03

Figure S37. ^{1}H NMR spectra for complexation of (*R*)-mandelic acid (*R*)-**3** in (**GluR**)$_2$ (1 : 1 guest : host ratio, (D-**GluR**)$_2$ middle, (L-**GluR**)$_2$ bottom) and the titration curves (400 MHz, 303 K, D_2O, pD 4.8, NaOD / DCl).

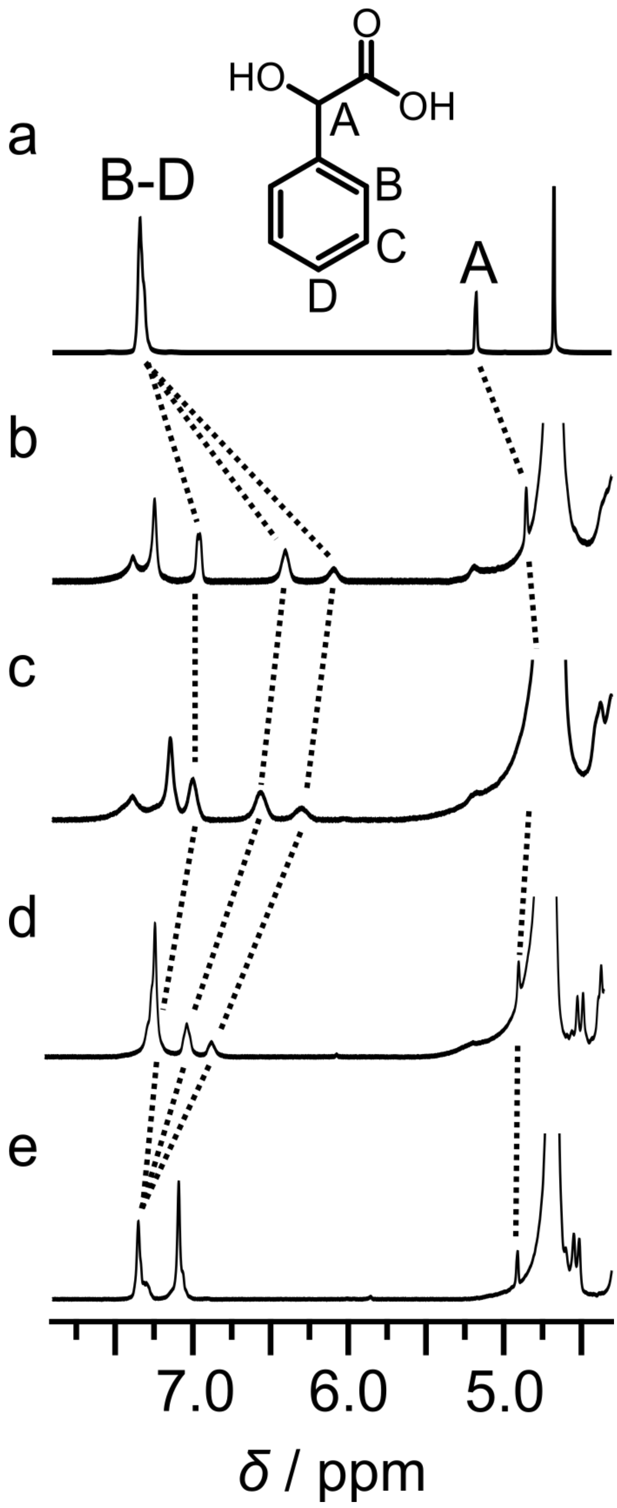

Figure S38. ^{1}H NMR spectra for complexation of (*R*)-mandelic acid (*R*)-**3** in (L-**GluR**)$_2$ (1 : 1 guest : host ratio) at various pD: a) (*R*)-**3** b) (L-**GluR**)$_2$ + (*R*)-**3** pD 4.5 c) (L-**GluR**)$_2$ + (*R*)-**3** pD 5.4 d) (L-**GluR**)$_2$ + (*R*)-**3** pD 9.1 e) (L-**GluR**)$_2$ + (*R*)-**3** pD 12.0 (400 MHz, 303 K, D_2O, NaOD / DCl).

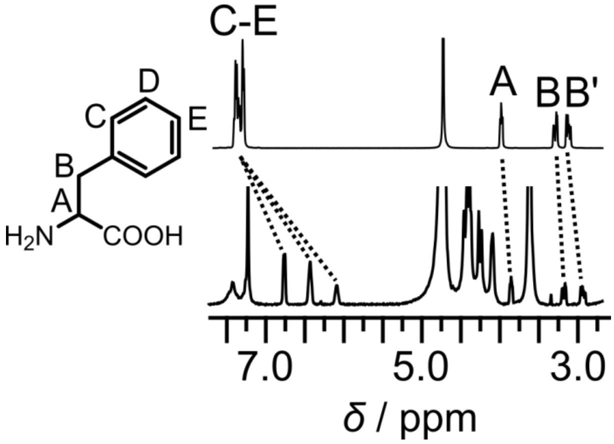

Figure S39. ^{1}H NMR spectra for complexation of phenylalanine **4** in (L-**GluR**)$_2$ (1 : 1 guest : host ratio, 400 MHz, 303 K, pD 4.8, D_2O, NaOD / DCl).

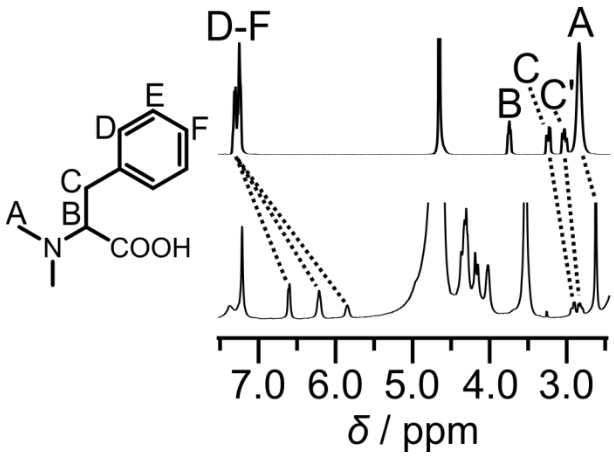

Figure S40. ^{1}H NMR spectra for complexation of *N*,*N*-dimethylphenylalanine **5** in (L-**GluR**)$_2$ (1 : 1 guest : host ratio, 400 MHz, 303 K, pD 4.8, D_2O, NaOD / DCl).

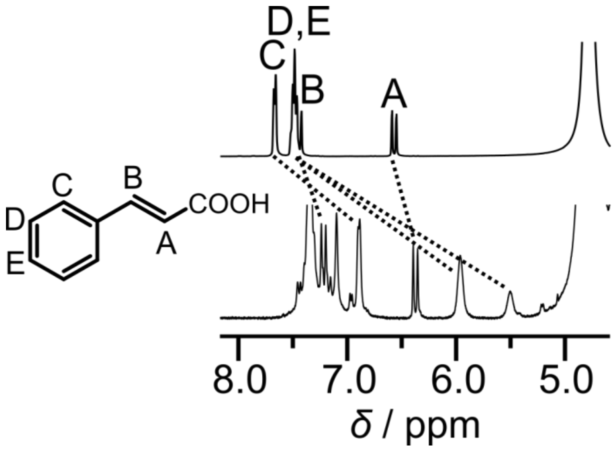

Figure S41. ^{1}H NMR spectra for complexation of cinnamic acid **6** in (L-**GluR**)$_2$ (1 : 1 guest : host ratio, 400 MHz, 303 K, pD 4.8, D_2O, NaOD / DCl).

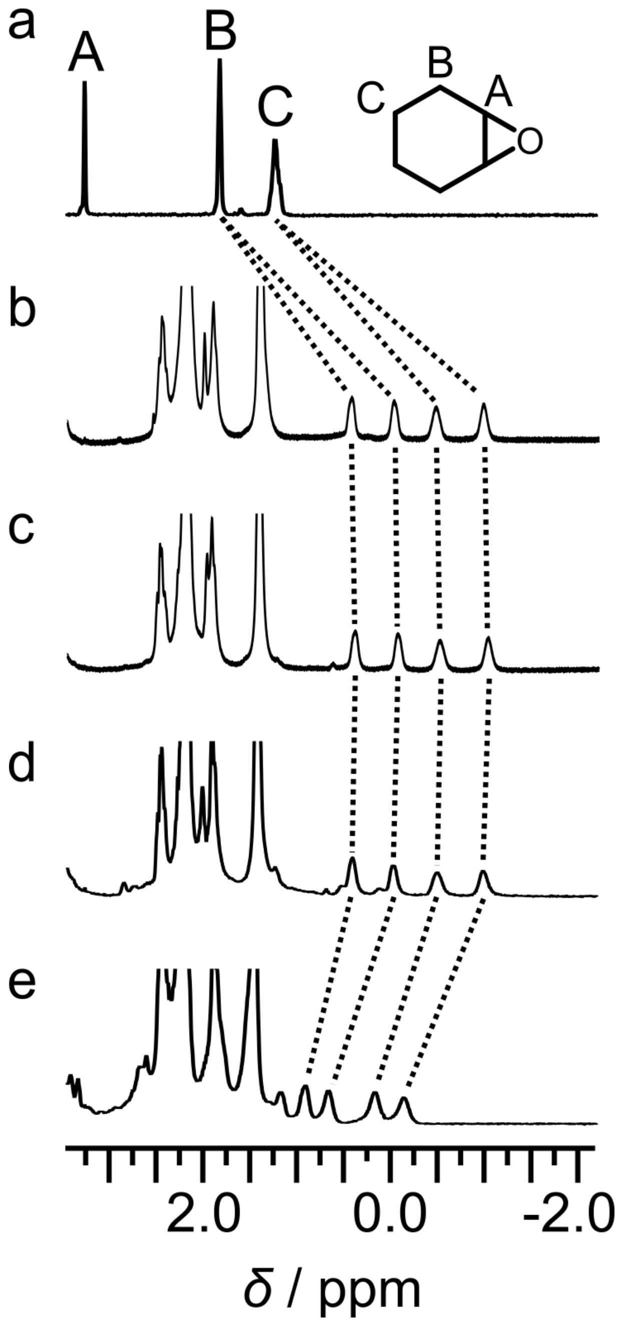

Figure S42. ^{1}H NMR spectra for complexation of epoxycyclohexane **7** in (L-**GluR**)$_2$: a) epoxycyclohexane; b) epoxycyclohexane + (L-**GluR**)$_2$ at pD 4.7 c) epoxycyclohexane + (L-**GluR**)$_2$ at pD 7.0 d) epoxycyclohexane + (L-**GluR**)$_2$ at pD 8.5 e) epoxycyclohexane + (L-**GluR**)$_2$ at pD 12.0 (1:1 guest : host ratio, 400 MHz, 303 K, D_2O, NaOD / DCl).

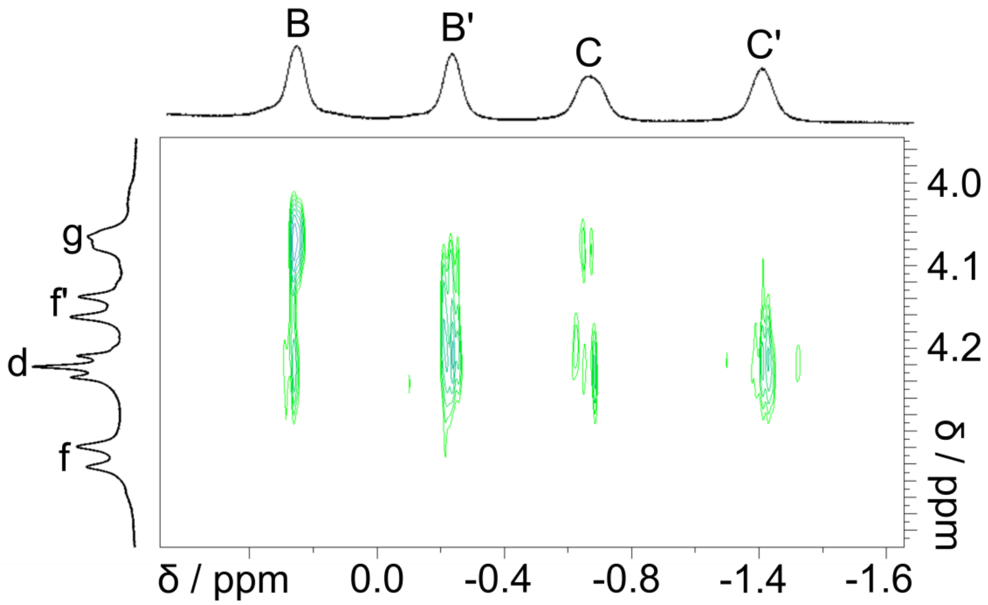

Figure S43. Partial ROESY spectrum of epoxycyclohexane in (L-**GluR**)$_2$ (600 MHz, 298 K, pD 4.8, D_2O, NaOD / DCl).

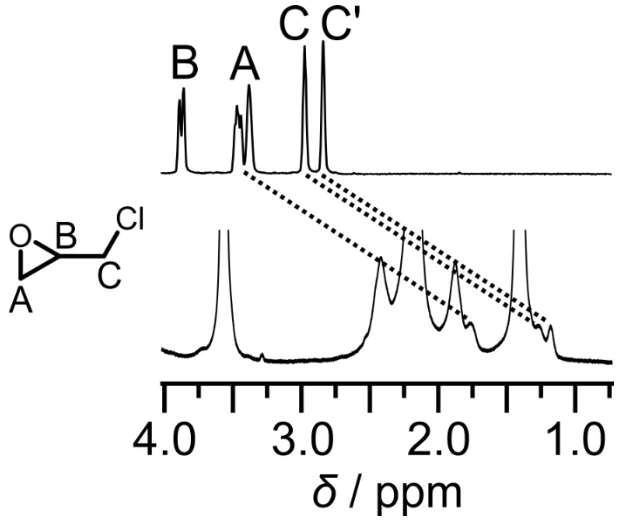

Figure S44. ^{1}H NMR spectra for complexation of epichlorohydrin **8** in (L-**GluR**)$_2$ (1 : 1 guest : host ratio, 400 MHz, 303 K, pD 4.8, D_2O, NaOD / DCl).

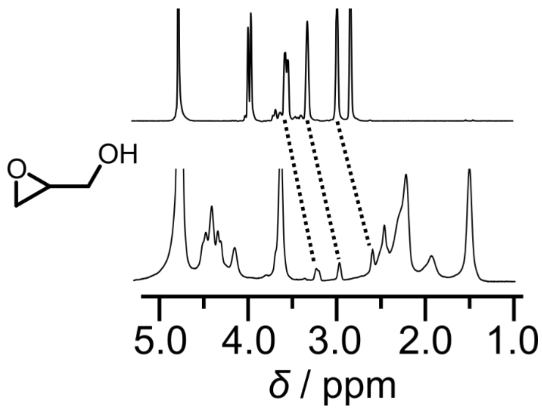

Figure S45. ^{1}H NMR spectra for complexation of glycidiol **9** in (L-**GluR**)$_2$ (1 : 1 guest : host ratio, 400 MHz, 303 K, pD 4.8, D_2O, NaOD / DCl).

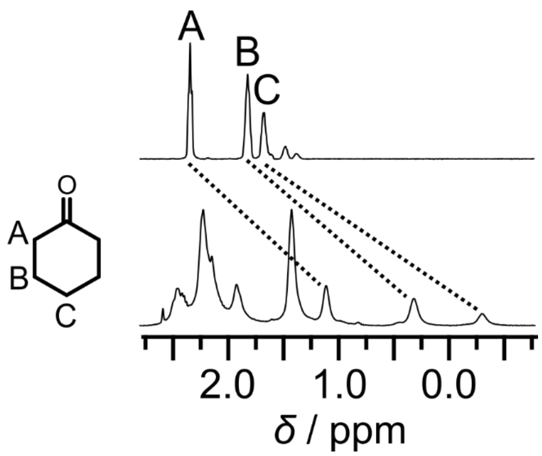

Figure S46. ^{1}H NMR spectra for complexation of cyclohexanone **10** in (L-**GluR**)$_2$ (1 : 1 guest : host ratio, 400 MHz, 303 K, pD 4.8, D_2O, NaOD / DCl).

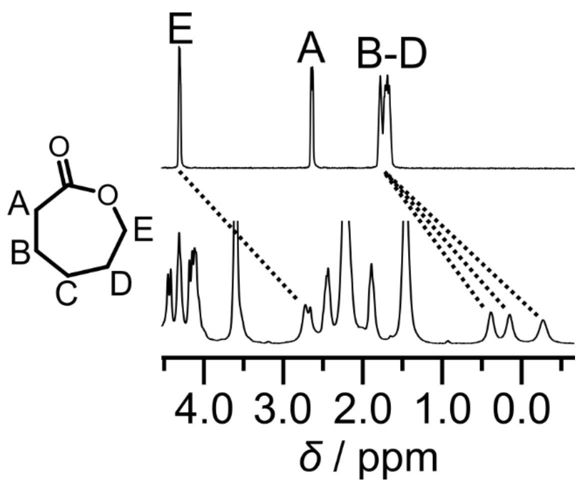

Figure S47. ^{1}H NMR spectra for complexation of caprolactone **11** in (L-**GluR**)$_2$ (1 : 1 guest : host ratio, 400 MHz, 303 K, pD 4.8, D_2O, NaOD / DCl).

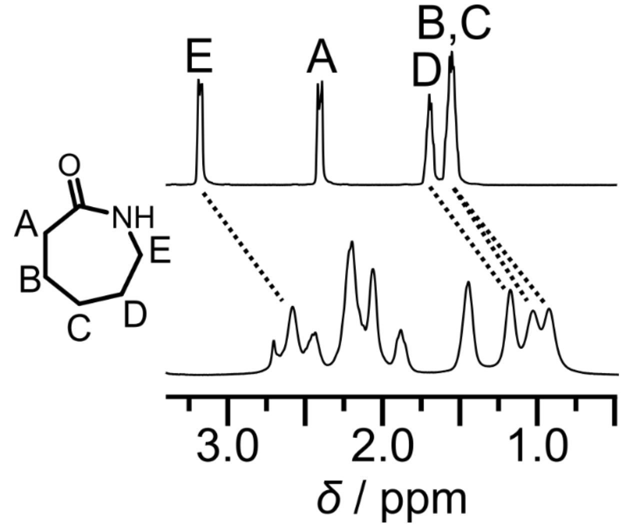

Figure S48. [1]H NMR spectra for complexation of caprolactam **12** in (L-**GluR**)$_2$ (1 : 1 guest : host ratio, 400 MHz, 303 K, pD 4.8, D_2O, NaOD / DCl).

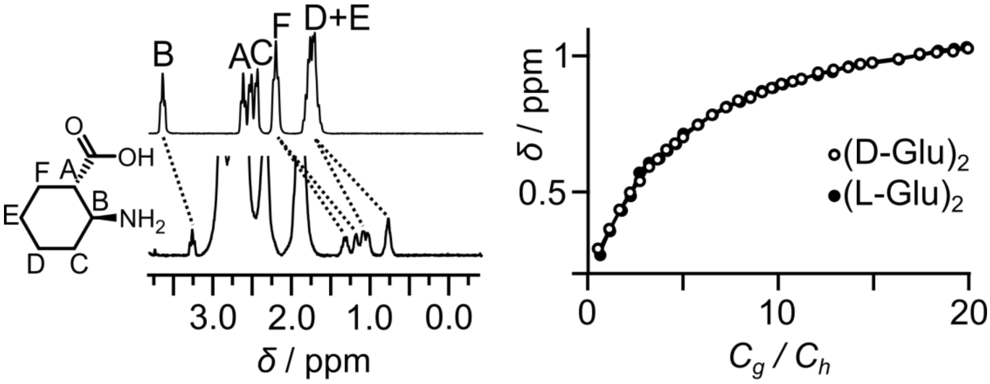

$$(\mathbf{GluR})_2 + \mathbf{13} \underset{}{\overset{K_1}{\rightleftharpoons}} (\mathbf{GluR})_2\mathbf{13}$$

$$(\mathbf{GluR})_2\mathbf{13} + \mathbf{13} \underset{}{\overset{K_2}{\rightleftharpoons}} (\mathbf{GluR})_2(\mathbf{13})_2$$

	K_1	σ_1	K_2	σ_2
(D-**GluR**)$_2$+(*R*)-**13**	4.80	0.02	1.46	0.02
(L-**GluR**)$_2$+(*R*)-**13**	4.80	0.05	1.32	0.05

Figure S49. [1]H NMR spectra for complexation of (1*S*,2*S*)-2-aminocyclohexanecarboxylic acid **13** in (**GluR**)$_2$ (1 : 1 guest : host ratio) and the titration curves (400 MHz, 303 K, pD 4.8, D_2O).

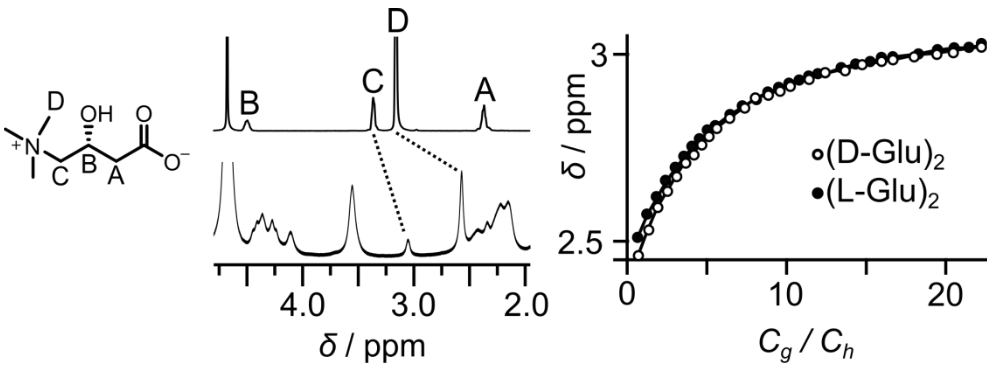

$$(\mathbf{GluR})_2 + \mathbf{14} \xrightleftharpoons{K_1} (\mathbf{GluR})_2\mathbf{14}$$

$$(\mathbf{GluR})_2\mathbf{14} + \mathbf{14} \xrightleftharpoons{K_2} (\mathbf{GluR})_2(\mathbf{14})_2$$

	K_1	σ_1	K_2	σ_2
(D-**GluR**)$_2$+(*R*)-**14**	4.77	0.03	1.54	0.03
(L-**GluR**)$_2$+(*R*)-**14**	4.99	0.02	1.43	0.02

Figure S50. ^{1}H NMR spectra for complexation of L-carnitine **14** in (**GluR**)$_2$ (1 : 1 guest : host ratio) and the titration curves (400 MHz, 303 K, pD 4.8, D_2O).

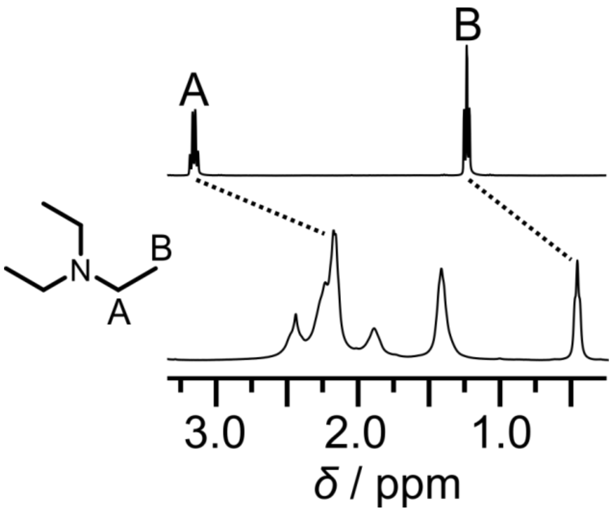

Figure S51. ^{1}H NMR spectra for complexation of trimethylamine **15** in (L-**GluR**)$_2$ (1 : 1 guest : host ratio, 400 MHz, 303 K, pD 4.8, D_2O, NaOD / DCl).

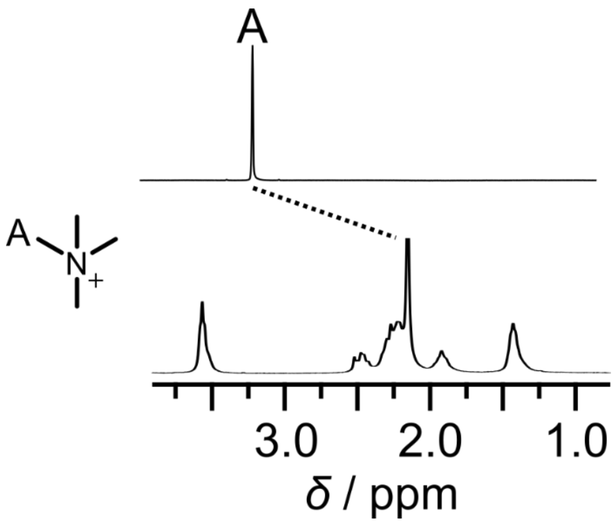

Figure S52. ^{1}H NMR spectra for complexation of tertamethylammonium salt **16** in (L-**GluR**)$_2$ (1 : 1 guest : host ratio, 400 MHz, 303 K, pD 4.8, D_2O, NaOD / DCl).

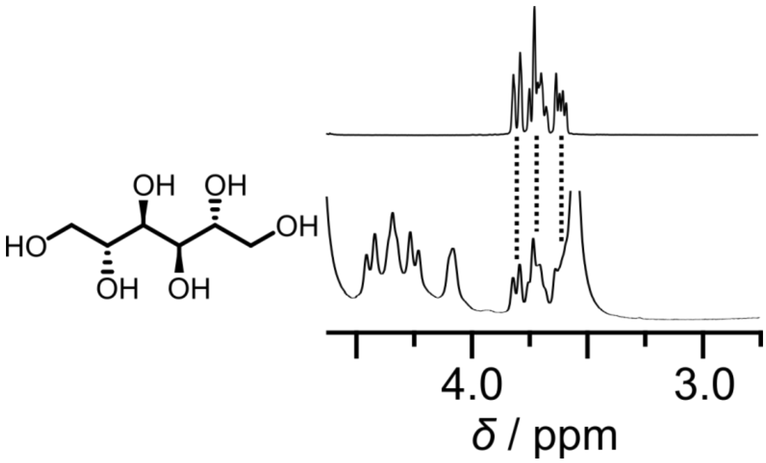

Figure S53. ^{1}H NMR spectra for complexation of mannitol in (L-**GluR**)$_2$ (1 : 1 guest : host ratio, 400 MHz, 303 K, pD 4.8, D_2O, NaOD / DCl).

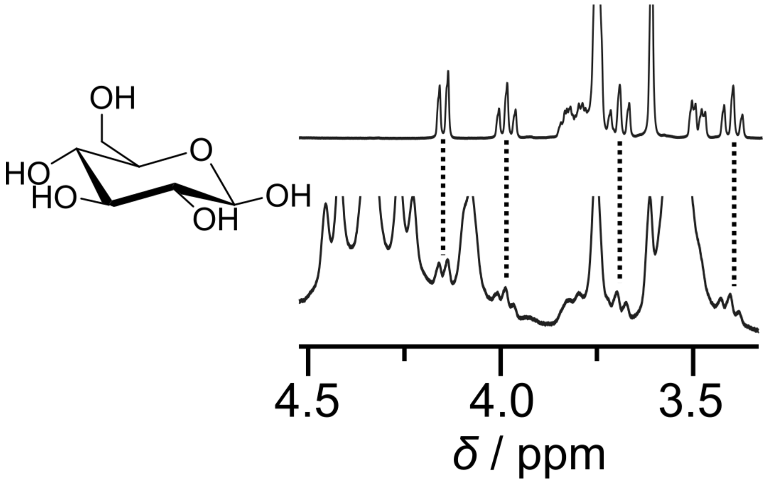

Figure S54. ^{1}H NMR spectra for complexation of glucose in (L-**GluR**)$_2$ (1 : 1 guest : host ratio, 400 MHz, 303 K, pD 4.8, D_2O, NaOD / DCl).

3. UV and ECD spectra

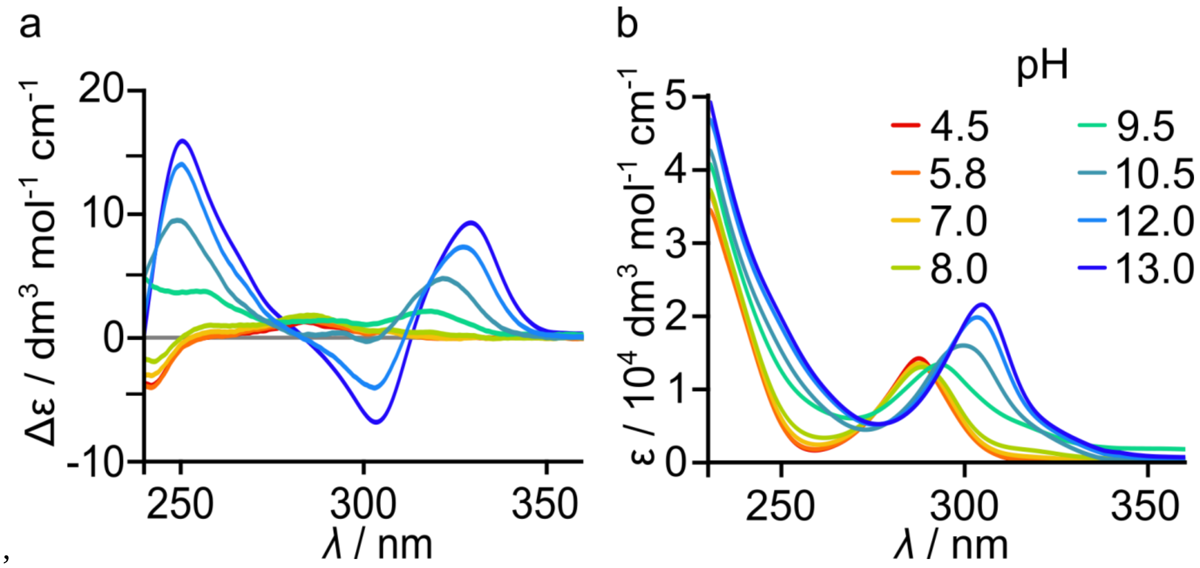

Figure S55. pH-dependent a) ECD and b) UV spectra of L-**GluR** (C = 3.1 mM concentration calculated per cavitand, water, pH set by NaOH / HCl).

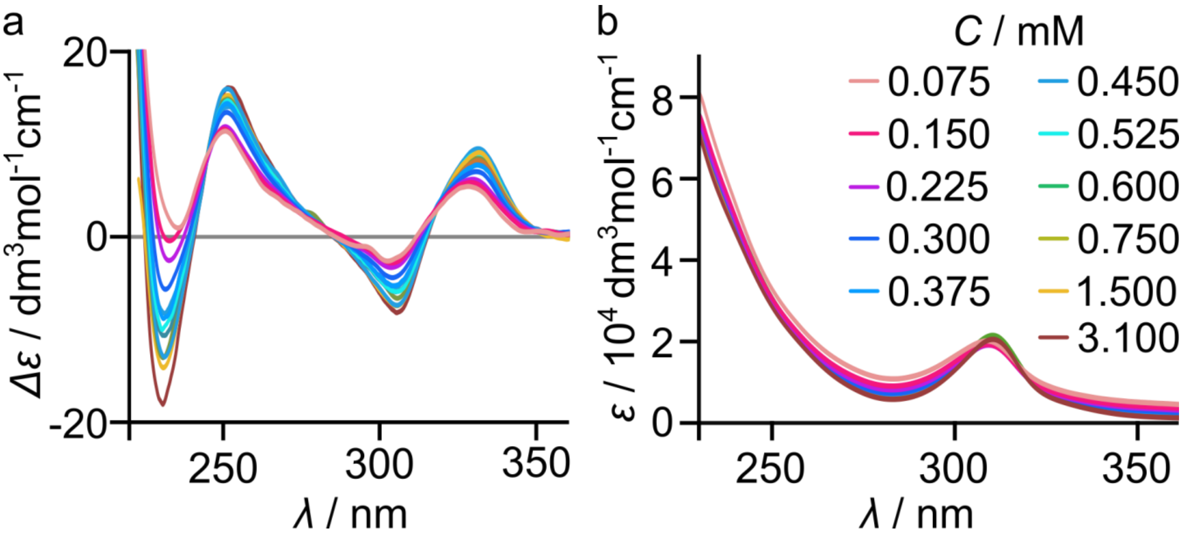

Figure S56. a) ECD and b) UV spectra of titration of L-**GluR** (concentration calculated per cavitand, water, pH = 11.90 pH set by NaOH / HCl).

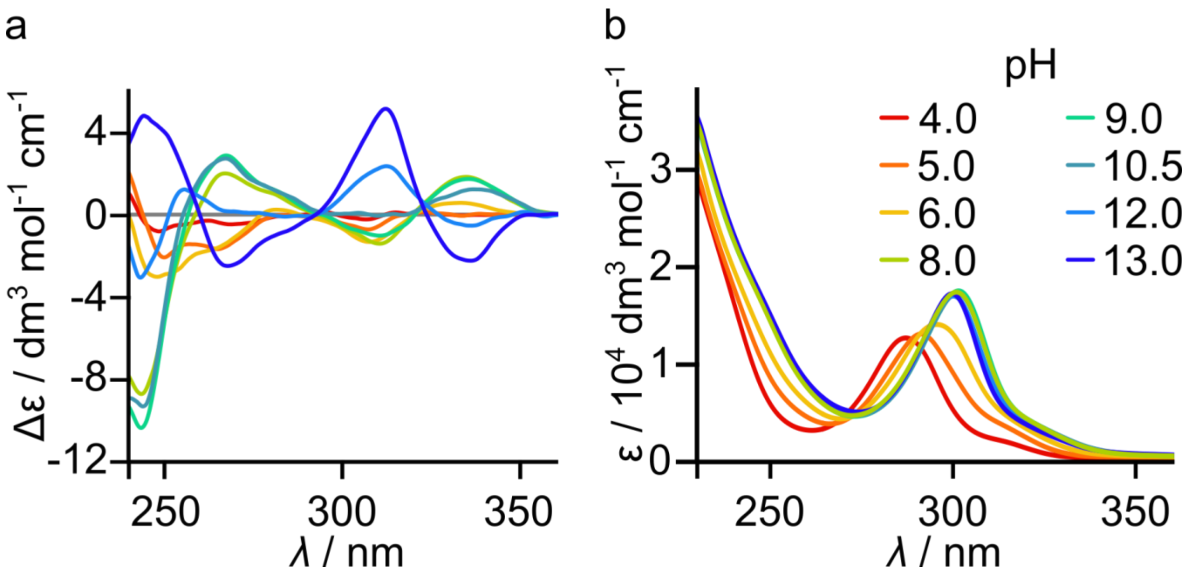

Figure S57. pH-dependent a) ECD and b) UV spectra of L-**ArgR** (C = 3.1 mM concentration calculated per cavitand, water, pH set by NaOH / HCl).

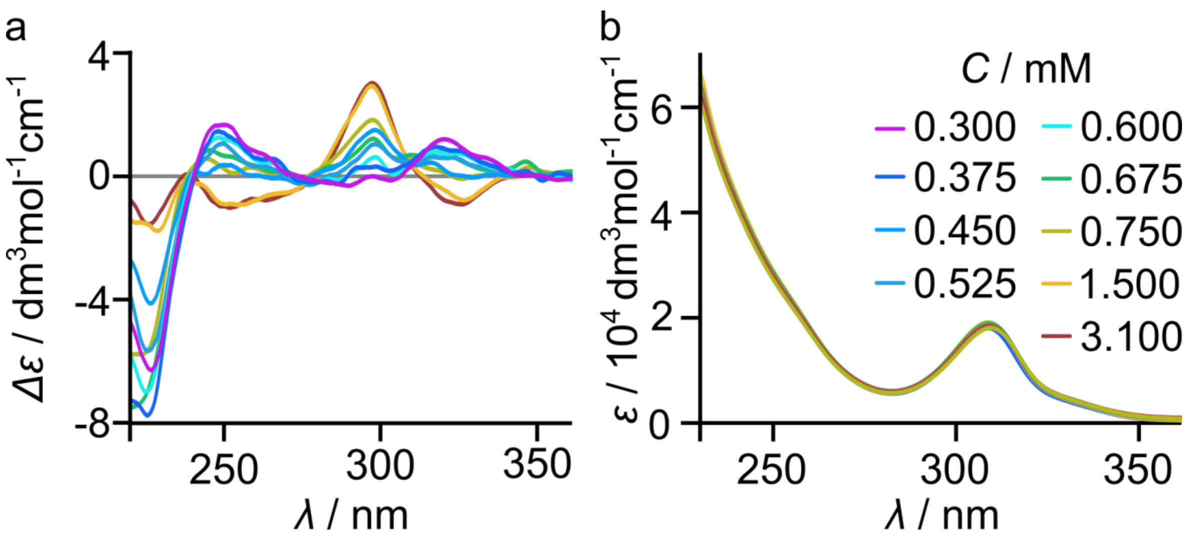

Figure S58. a) ECD and b) UV spectra of titration of L-**ArgR** (concentration calculated per cavitand, water, pH = 11.90 pH set by NaOH / HCl).

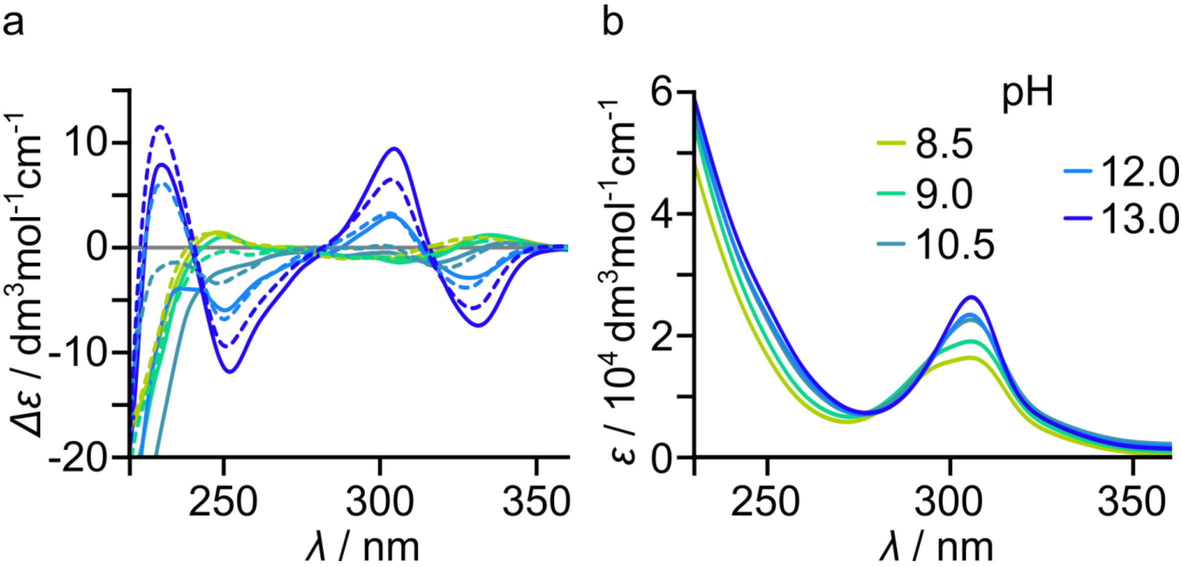

Figure S59. pH-dependent a) ECD and b) UV spectra of D-**GluR**-D-**ArgR** (solid lines – experimental spectra, dashed lines – a weighted mathematical sum of the components at given pH) ($C_{(\text{L-}\mathbf{ArgR})}$ = 1.85 mM, $C_{(\text{D-}\mathbf{GluR})}$ = 1.85 mM, water, pH set by NaOH / HCl).

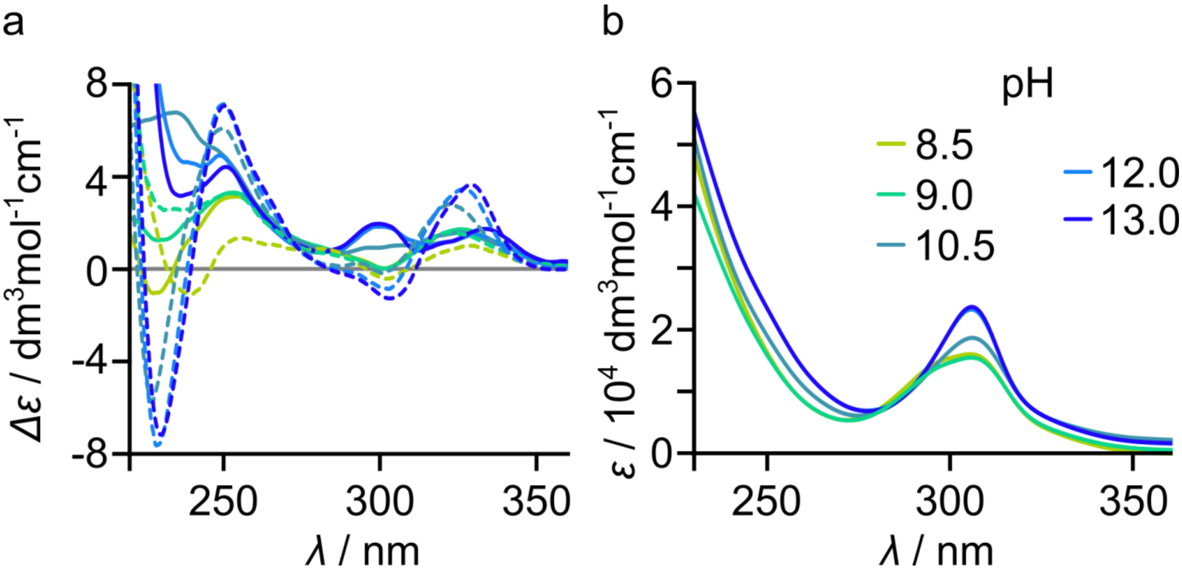

Figure S60. pH-dependent a) ECD and b) UV spectra of L-**GluR**-L-**ArgR** (solid lines – experimental spectra, dashed lines – a weighted mathematical sum of the components at given pH) ($C_{(\text{L-}\mathbf{ArgR})}$ = 1.85 mM, $C_{(\text{L-}\mathbf{GluR})}$ = 1.85 mM, water, pH set by NaOH / HCl).

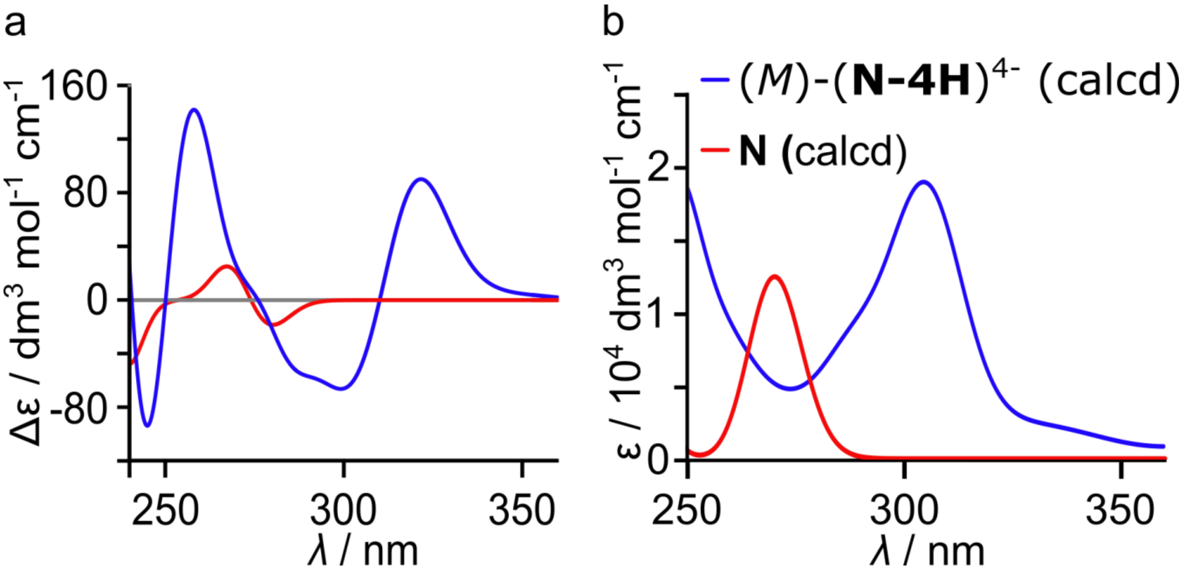

Figure S61. Calculated a) ECD and b) UV spectra of (*M*)-(**N-4H**)$^{4-}$ and **N**.

4. IR spectra

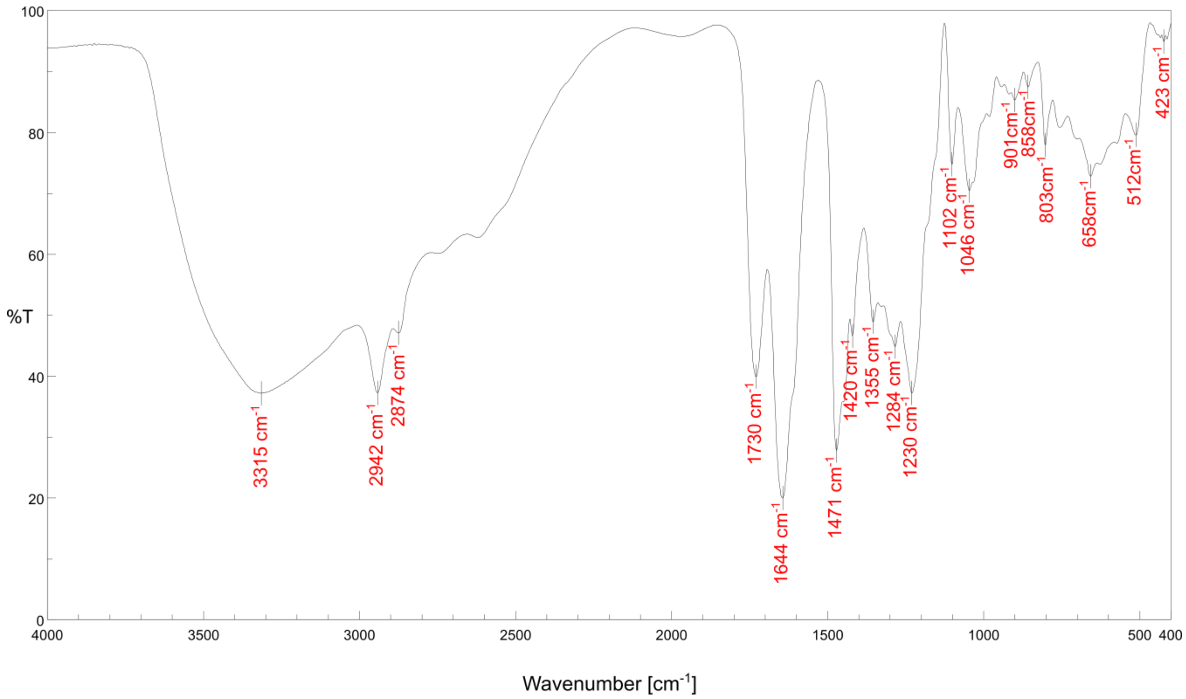

Figure S62. IR spectrum of L-**GluR** (KBr).

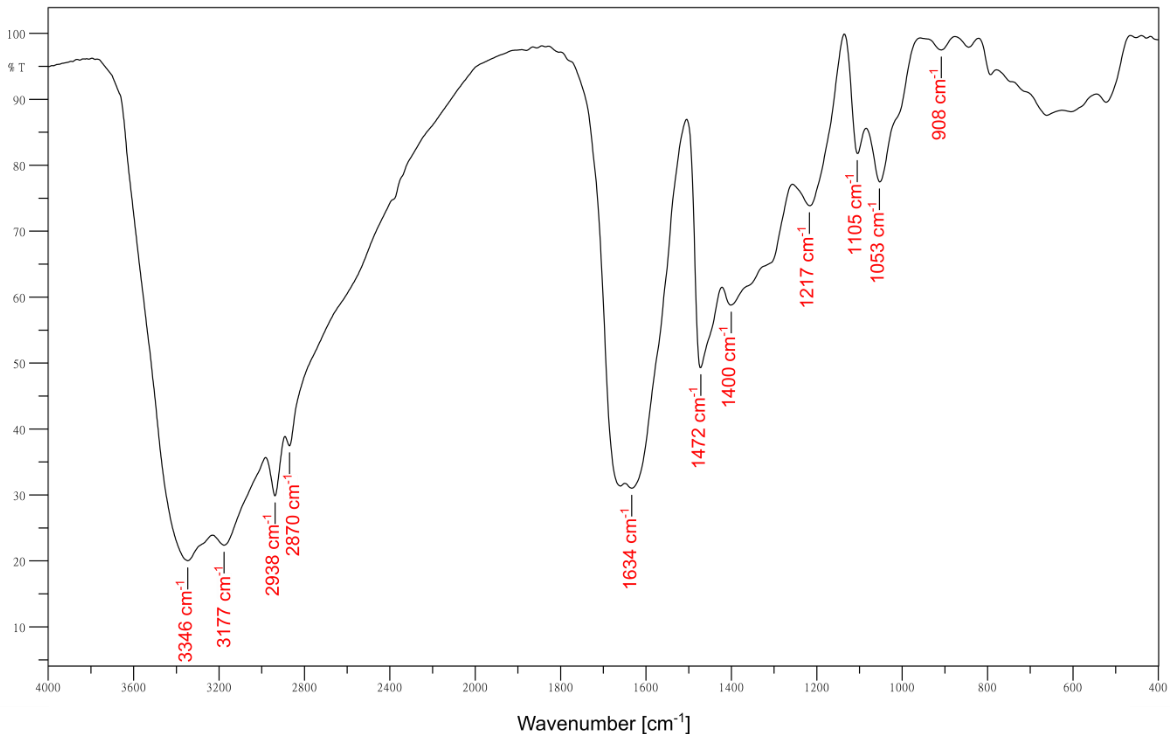

Figure S63. IR spectrum of L-**ArgR** (KBr).

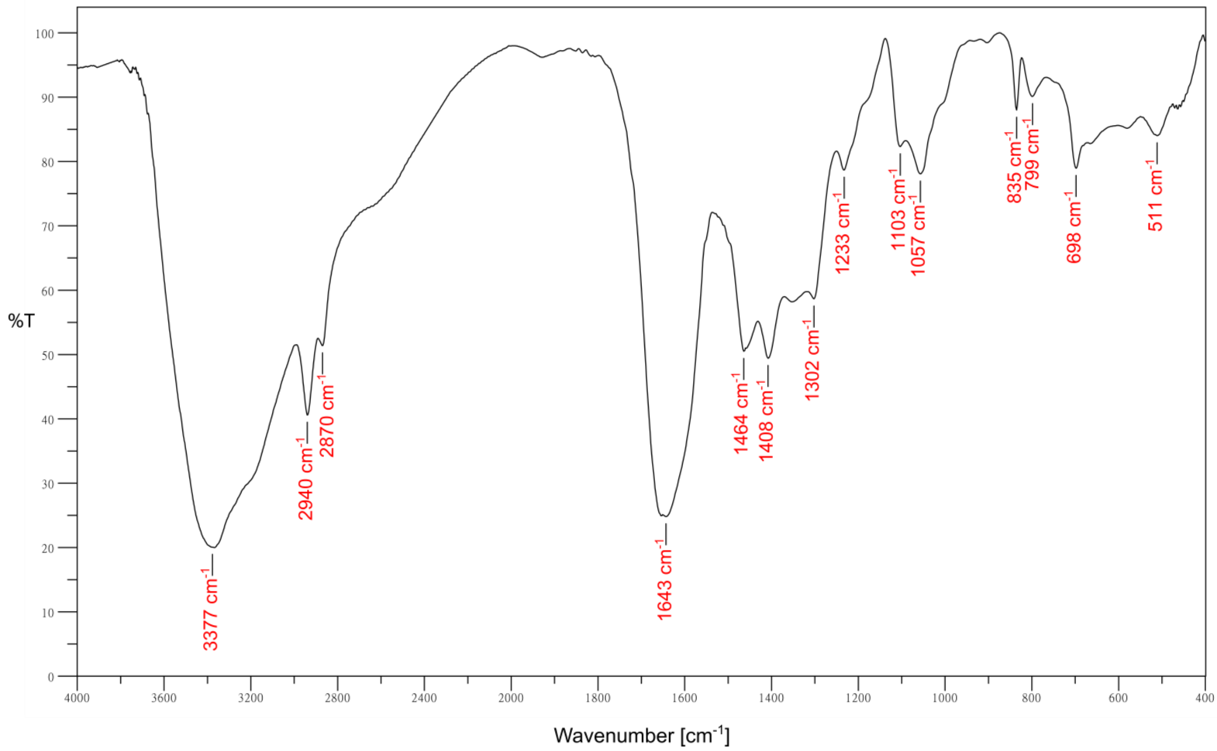

Figure S64. IR spectrum of D-**GluR**-L-**ArgR** (KBr).

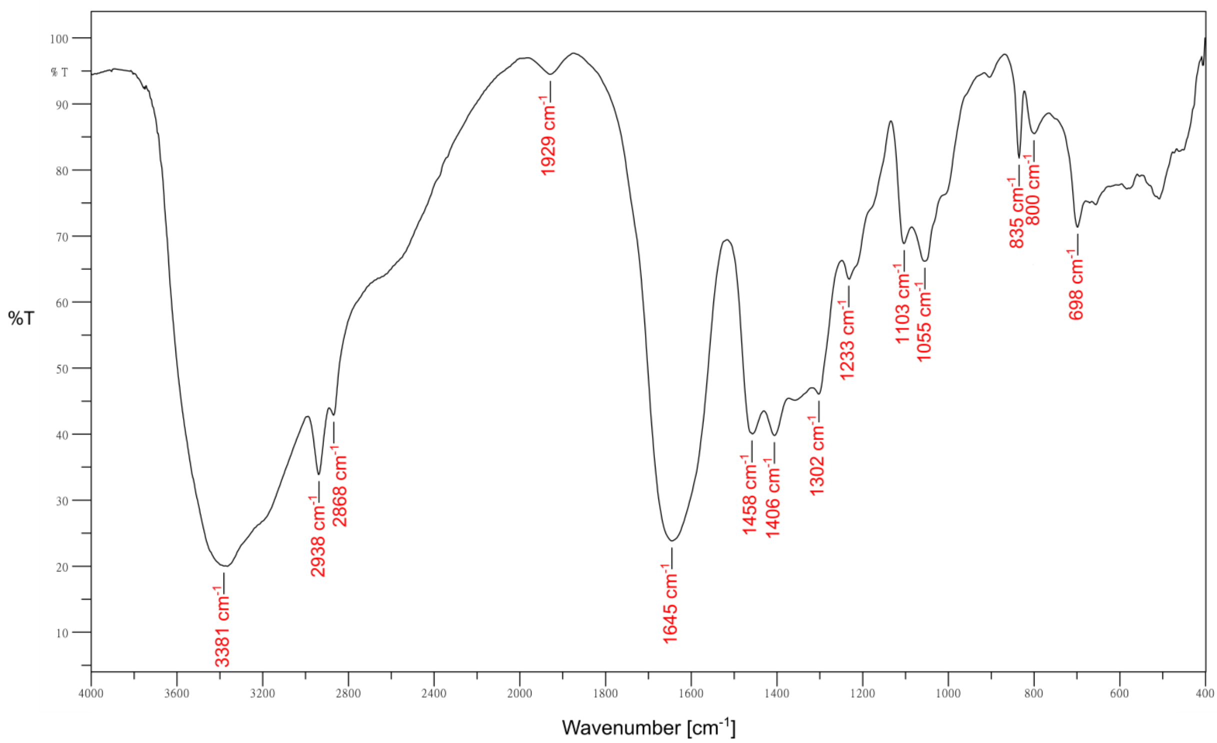

Figure S65. IR spectrum of L-**GluR**-L-**ArgR** (KBr).

5. MS spectra

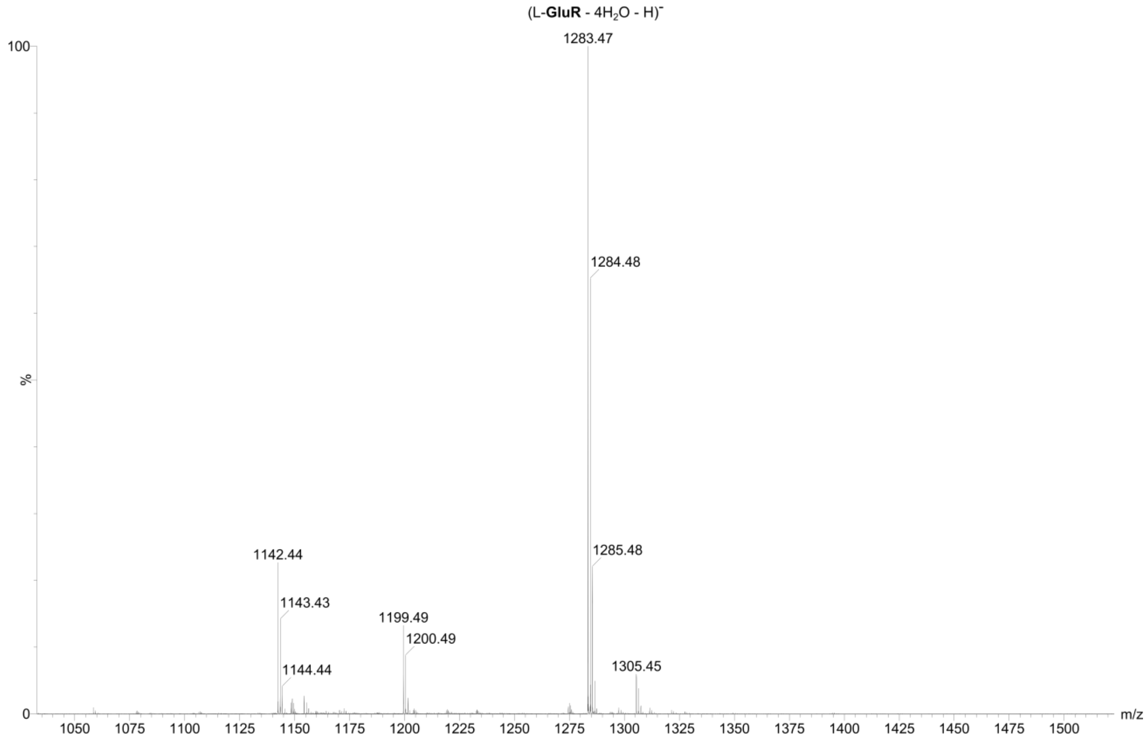

Figure S66 TOF-ESI of L-**GluR**.

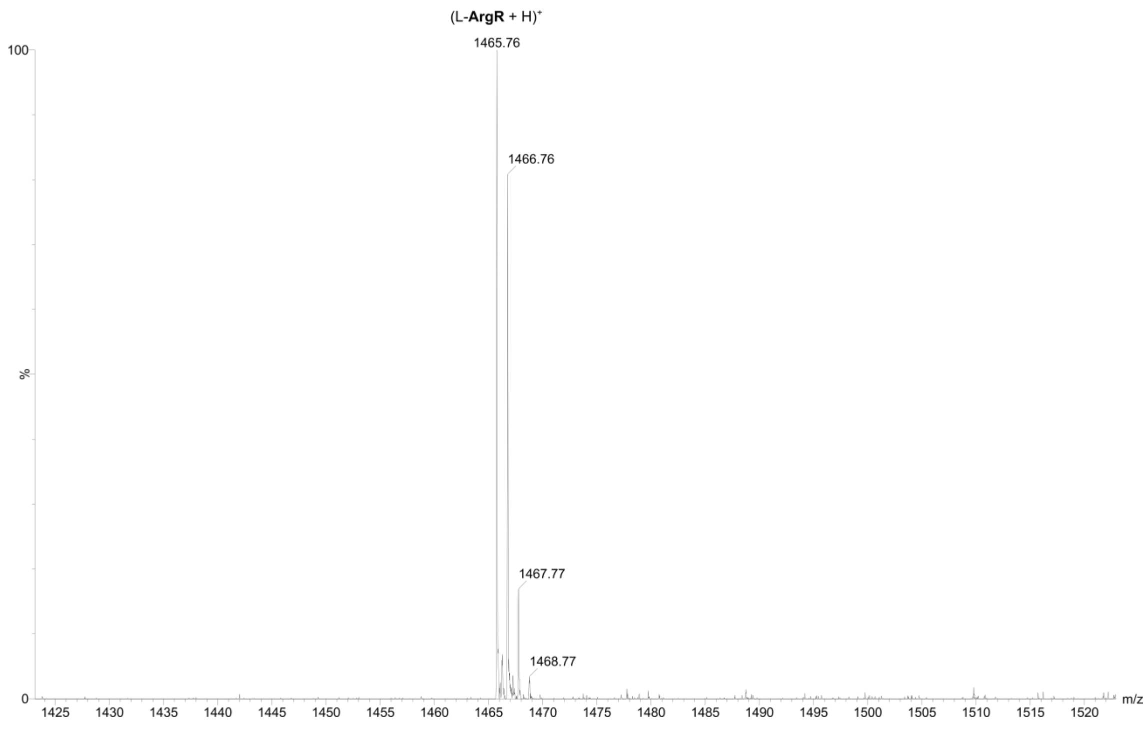

Figure S67. TOF-ESI of L-**ArgR**.

6. Calculations of the size of the capsule

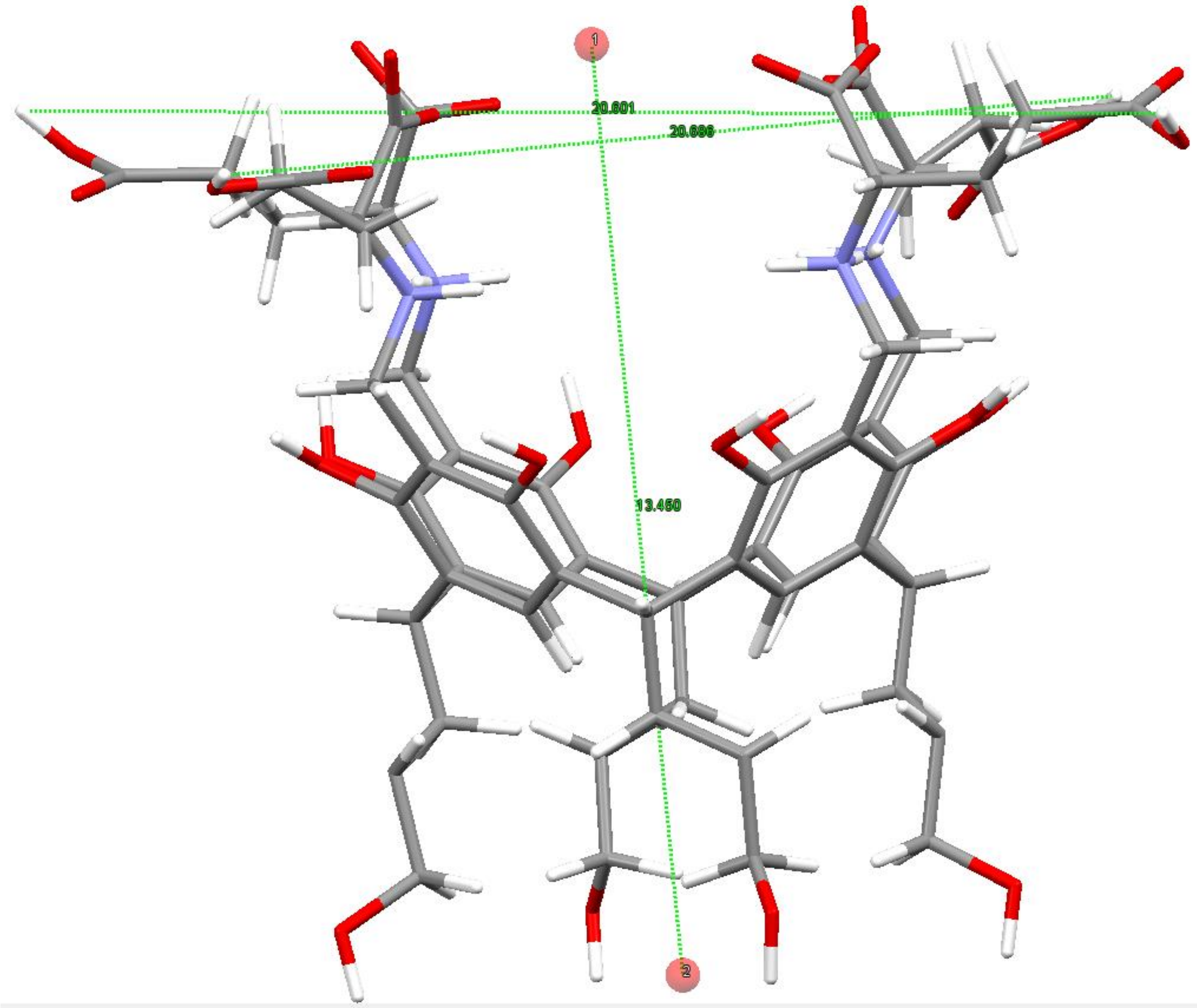

$$\bar{x}_r = \frac{20.601 + 20.686 + 13.450}{6} = 9.12 \text{ Å}$$

Figure S68. Approximation of the average size of L-**GluR**.

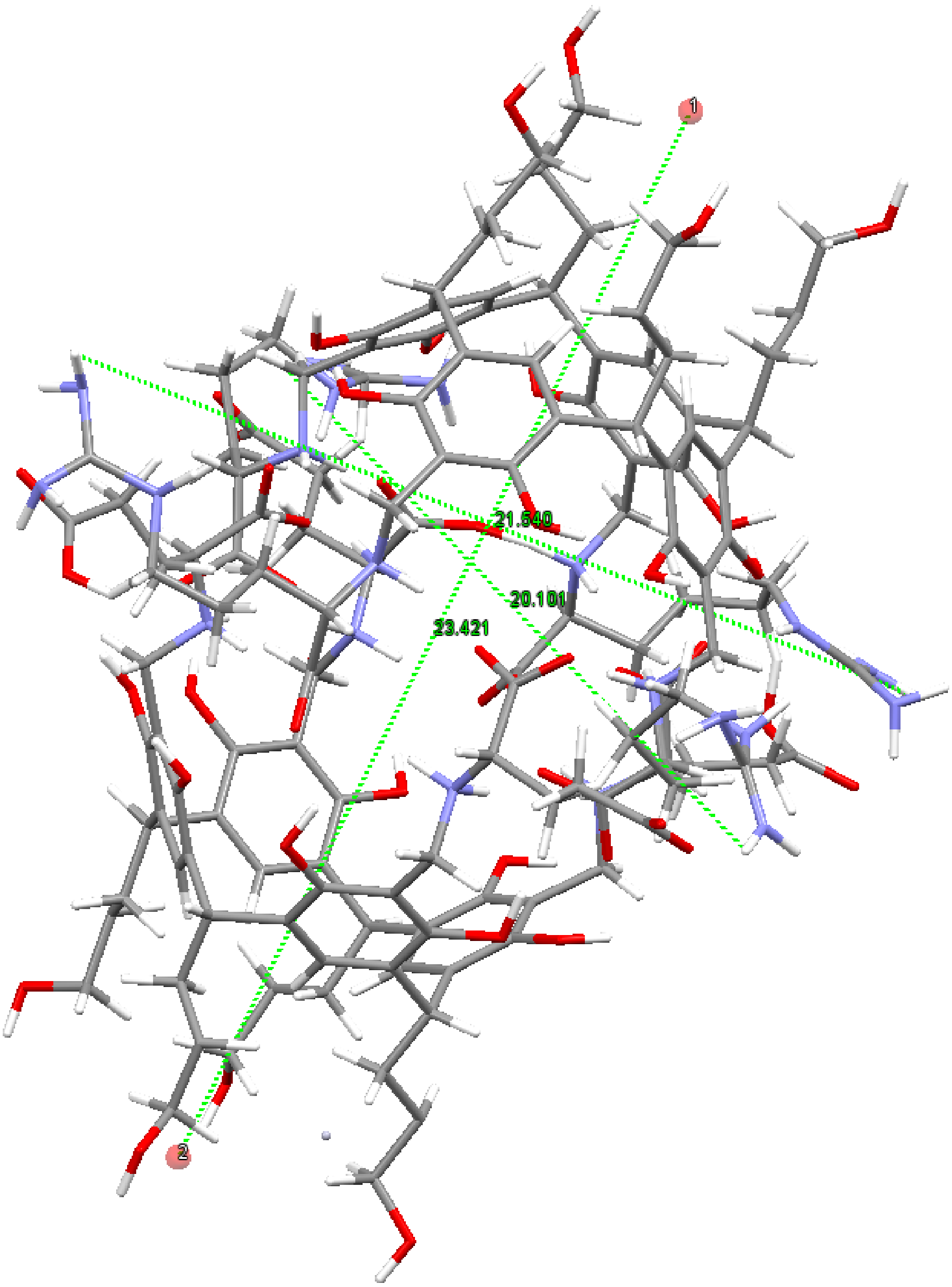

$$\bar{x}_r = \frac{23.421 + 20.101 + 21.540}{6} = 10.8 \text{ Å}$$

Figure S69. Approximation of the average size of L-**GluR**-L-**ArgR**.

[1] Gibb, B. C., Chapman, R. G., and Sherman, J. C. (1996). Synthesis of Hydroxyl-Footed Cavitands. *J. Org. Chem.*, 61, 1505-1509. doi.org/10.1021/jo951633c